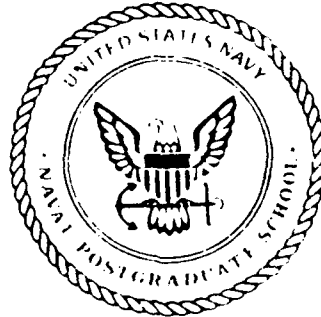


AD-A260 618



(2)

**NAVAL POSTGRADUATE SCHOOL**  
**Monterey, California**



**DTIC**  
**ELECTE**  
**FEB 23 1993**  
**S C D**

**THESIS**

ORBITAL PARAMETER ESTIMATION USING AN  
EXTENDED KALMAN FILTER

by

Daniel J. Brett

December 1992

Thesis Advisor:

Harold A. Titus

Approved for public release; distribution is unlimited

**93-03609**

251450 10408

Unclassified

SECURITY CLASSIFICATION OF THIS PAGE

REPORT DOCUMENTATION PAGE				Form Approved OMB No. 0704-0188	
1a. REPORT SECURITY CLASSIFICATION <b>Unclassified</b>			1b. RESTRICTIVE MARKINGS		
2a. SECURITY CLASSIFICATION AUTHORITY			3. DISTRIBUTION/AVAILABILITY OF REPORT Approved for public release; distribution is unlimited		
2b. DECLASSIFICATION/DOWNGRADING SCHEDULE					
4. PERFORMING ORGANIZATION REPORT NUMBER(S)			5. MONITORING ORGANIZATION REPORT NUMBER(S)		
6a. NAME OF PERFORMING ORGANIZATION <b>Naval Postgraduate School</b>		6b. OFFICE SYMBOL (If applicable)	7a. NAME OF MONITORING ORGANIZATION <b>Naval Postgraduate School</b>		
6c. ADDRESS (City, State, and ZIP Code) <b>Monterey, CA 93943-5000</b>			7b. ADDRESS (City, State, and ZIP Code) <b>Monterey, CA 93943-5000</b>		
8a. NAME OF FUNDING/SPONSORING ORGANIZATION		8b. OFFICE SYMBOL (If applicable)	9. PROCUREMENT INSTRUMENT IDENTIFICATION NUMBER		
8c. ADDRESS (City, State, and ZIP Code)			10. SOURCE OF FUNDING NUMBERS		
PROGRAM ELEMENT NO.		PROJECT NO.	TASK NO.	WORK UNIT ACCESSION NO.	
11. TITLE (Include Security Classification) <b>ORBITAL PARAMETER ESTIMATION USING AN EXTENDED KALMAN FILTER</b>					
12. PERSONAL AUTHOR(S) <b>Daniel J. Brett</b>					
13a. TYPE OF REPORT <b>Doctoral Dissertation</b>		13b. TIME COVERED FROM _____ TO _____	14. DATE OF REPORT (Year, Month, Day) <b>December 1992</b>		15. PAGE COUNT <b>108</b>
16. SUPPLEMENTARY NOTATION The views expressed in this thesis are those of the author and do not reflect the official policy or position of the Department of Defense or the U.S. Government.					
17. COSATI CODES			18. SUBJECT TERMS (Continue on reverse if necessary and identify by block number)		
FIELD	GROUP	SUB-GROUP			
			Kalman Filter, Orbital Elements, Coordinate Transformation, Radar Plane, Direction Cosines.		
19. ABSTRACT (Continue on reverse if necessary and identify by block number) The problem of orbital parameter estimation using angles only observations is examined. Direction cosine measurements, obtained from satellite passage of an earth-based stationary planar radar beam, are assimilated by an extended Kalman filter to improve estimates of a classical orbital element set. Several progressively comprehensive orbital motion models are considered and compared. The relative effectiveness of these models is illustrated by applying them to actual satellite data.					
20. DISTRIBUTION/AVAILABILITY OF ABSTRACT <input checked="" type="checkbox"/> UNCLASSIFIED/UNLIMITED <input type="checkbox"/> SAME AS RPT. <input type="checkbox"/> DTIC USERS			21. ABSTRACT SECURITY CLASSIFICATION <b>Unclassified</b>		
22a. NAME OF RESPONSIBLE INDIVIDUAL <b>Harold A. Titus</b>			22b. TELEPHONE (Include Area Code) <b>(408) 646 - 2560</b>		22c. OFFICE SYMBOL <b>EC/Ts</b>

DD Form 1473, JUN 86

Previous editions are obsolete.  
S/N 0102-LF-014-6603SECURITY CLASSIFICATION OF THIS PAGE  
Unclassified

Approved for public release; distribution is unlimited.

Orbital Parameter Estimation Using an Extended Kalman Filter

by

Daniel J. Brett  
Captain, United States Air Force  
B.S., South Dakota School of Mines and Technology, 1981  
M.S., Air Force Institute of Technology, 1983

Submitted in partial fulfillment of the requirements for  
the degree

DOCTOR OF PHILOSOPHY IN ELECTRICAL ENGINEERING

from the

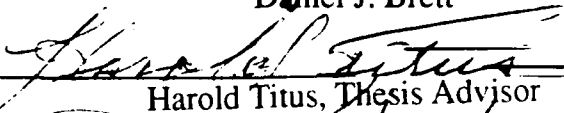
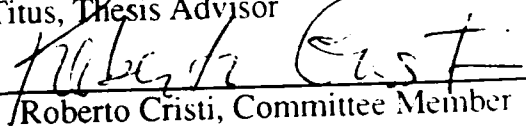
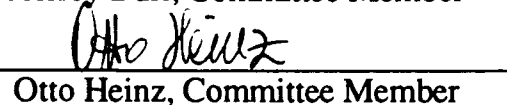
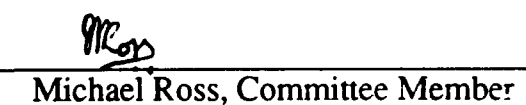
NAVAL POSTGRADUATE SCHOOL  
December 1992

Author:

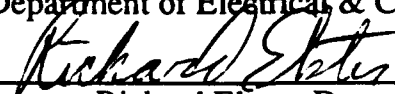


Daniel J. Brett

Approved by:

  
Harold Titus, Thesis Advisor  
Jeffrey Burl, Committee Member  
Roberto Cristi, Committee Member  
Otto Heinz, Committee Member  
Michael Ross, Committee Member

Michael A. Morgan, Chairman,  
Department of Electrical & Computer Engineering



Richard Elster, Dean of Instruction

## ABSTRACT

The problem of orbital parameter estimation using angles only observations is examined. Direction cosine measurements, obtained from satellite passage of an earth-based stationary planar radar beam, are assimilated by an extended Kalman filter to improve estimates of a classical orbital element set. Several progressively comprehensive orbital motion models are considered and compared. The relative effectiveness of these models is illustrated by applying them to actual satellite data.

DTIC QUALITY INSPECTED 3

Accession For	
NTIS CRA&I	<input checked="checked" type="checkbox"/>
DTIC TAB	<input type="checkbox"/>
Unannounced	<input type="checkbox"/>
Justification	
By	
Distribution /	
Availability Codes	
Dist	Avail and/or Special
A-1	

## TABLE OF CONTENTS

<b>I. INTRODUCTION.....</b>	<b>1</b>
<b>II. REVIEW OF LITERATURE.....</b>	<b>2</b>
<b>III. TWO-BODY ORBIT FORMULATION .....</b>	<b>4</b>
A. KEPLER TWO-BODY DYNAMICS .....	4
B. OBSERVATIONS .....	9
C. RADAR PLANE INTERSECTION .....	15
<b>IV. DOMINANT PERTURBATIONS .....</b>	<b>18</b>
A. GRAVITY PERTURBATIONS .....	18
B. DRAG PERTURBATIONS .....	24
1. Atmospheric Drag Effects.....	24
2. Simplified Drag Effects .....	26
3. Atmospheric Drag Characterization .....	28
<b>V. THE RECURSIVE ORBITAL PARAMETER ESTIMATOR .....</b>	<b>31</b>
A. FILTER INITIALIZATION .....	31
1. Input Data Files .....	33
2. Constants.....	34
3. Time .....	34
4. Filter Matrices.....	35
B. STATE PROPAGATION .....	35
C. RADAR PLANE INTERSECTION .....	36
D. ASSIMILATION OF OBSERVATIONS.....	38
<b>VI. RESULTS .....</b>	<b>42</b>
A. RADAR PLANE TIME OF ARRIVAL .....	42
B. RESIDUAL SMALL SAMPLE STATISTIC.....	44
C. ORBITAL PARAMETER ESTIMATION.....	45

VII. CONCLUSIONS AND RECOMMENDATIONS .....	52
LIST OF REFERENCES .....	53
APPENDIX A - COORDINATE TRANSFORMATIONS .....	55
APPENDIX B - LINEARIZED FILTER MATRICES $\hat{\Phi}$ AND $\hat{H}$ .....	62
APPENDIX C - FILTER CODE (MATLAB) .....	78
INITIAL DISTRIBUTION LIST .....	99

## FIGURES

Figure 3.1. Classical orbital elements. ....	5
Figure 3.2. Eccentric vs. true anomaly. ....	8
Figure 3.3. Radar plane geometry. ....	10
Figure 3.4. Receiver site geometry. ....	11
Figure 3.5. Receiver site geometry. ....	13
Figure 3.6. Radar plane orientation. ....	16
Figure 4.1. Satellite moving through perigee. ....	27
Figure 5.1. Estimator flow chart. ....	32
Figure 5.2. Sensor field of view. ....	38
Figure 6.1. Variance of residuals (sat. # 116). ....	46
Figure 6.2. Variance of residuals (sat. # 117). ....	47
Figure 6.3. Variance of residuals (sat. # 118). ....	48
Figure 6.4. Orbital element estimates (sat. # 116). ....	49
Figure 6.5. Orbital element estimates (sat. # 117). ....	50
Figure 6.6. Orbital element estimates (sat. # 118). ....	51
Figure A.1. Reference frames. ....	56
Figure A.2. Orbit-fixed to inertial rotations. ....	57
Figure A.3. Inertial to site-based rotations. ....	59
Figure A.4. Inertial to radar plane rotations. ....	61
Figure B.1. Site-based coordinate system. ....	69
Figure B.2. Relationship between satellite position and range. ....	70

## TABLES

Table 4.1. DRAG PARAMETERS. ....	30
Table 6.1. OBSERVED VS. ESTIMATED TIMES OF ARRIVAL. ....	43
Table B.1. DEVELOPMENT OF TERMS FOR $\hat{H}$ . ....	77

## **ACKNOWLEDGEMENTS**

I would like to thank God for His sustenance and my wife and son for their patience. My thanks also go to Dr. Hal Titus, my thesis advisor, for his guidance and encouragement throughout this undertaking. In addition, I wish to thank the members of my committee, Drs. Roberto Cristi, Jeffrey Burl, Otto Heinz, and Michael Ross, for their timely help and encouragement.

## I. INTRODUCTION

Earth-orbiting satellites are catalogued in the form of orbital element sets. For maximum usefulness of these catalogs to military and civil space systems, element sets need to be updated as frequently and as accurately as possible. A nonlinear filter was designed to perform these updates in near-real-time using observations of satellites piercing a planar radar beam.

The filter predicts time-varying orbital parameters according to a non-linear orbital dynamics model. This model includes, along with two-body Keplerian motion, first order oblateness effects, both secular and periodic, simple decreasing exponential atmospheric drag effects, and white noise on both the dynamic model and the measured observations. This simple model is found sufficient to track several selected satellites, with proper tuning of the filter. It should be noted that even this simple non-linear model gives rise to comparatively complex filter expressions.

Applying this filter to the orbit improvement problem helps meet the need for continual determination of orbit decay, collision avoidance, satellite maneuvers, etc. Current systems use a daily batch least squares differential correction method.

## II. REVIEW OF LITERATURE

This research involves the integration of a simple, yet adequate, orbital dynamics model with a necessarily suboptimal extended Kalman estimator. This combination is applied to a geometrically unique detection scheme to provide near real-time improvement of orbital elements for selected satellites. The accuracy level under consideration falls under the umbrella of the general perturbations problem of orbital mechanics, which is covered by numerous textbooks, a sampling of which are referred to here [1-6]. In general, solution procedures involve a gravitational potential function (earth oblateness, third body, etc.) describing its contribution to the perturbation of a classical two-body Keplerian dynamic model. The resultant expressions take the form of variations in some set of orbital parameters. The two broad divisions of orbital parameter representation in the literature are: 1) some set of 6 orbital elements which describe the orbital path as a conic section and its orientation in inertial space, and 2) Cartesian position and velocity of the orbiting body. The 6 classical orbital elements were chosen for their physical significance in terms of how the satellite's orbit is being affected by various perturbing forces. The particular satellite propagation theory being used here is loosely based on Brouwer's theory [7-11] for a future comparison basis with existing orbit improvement procedures. The detection scheme is an earth-fixed planar radar, the crossing of which causes power to be reflected back to one or more of multiple earth-based receivers [12].

The most poorly modeled phenomenon affecting low earth orbits is the problem of atmospheric drag. The overwhelming consensus [13-15] is that even the most complex atmospheric density models can only be consistently accurate to within about 20%. The Kalman filter incorporates a very simple decreasing exponential density model [16] corrupted by noise to track drag perturbations.

The extended Kalman filter is used in many situations for nonlinear parameter estimation [17-19] and has been applied to the field of orbit estimation in the form of orbital parameter improvement by differential correction techniques [20,21]. It is known that such a filter works well when observational data are plentiful [22,23]. However, proper application of such a filter to a highly nonlinear, minimal observation scenario, such as that posed by the fixed radar plane detection scheme, can also successfully "track" satellites.

### III. TWO-BODY ORBIT FORMULATION

Two-body orbital motion for a spherical earth can be described by a set of six parameters (three-dimensional, second order problem). Traditionally, these parameters take one of two forms. One method describes satellite motion in terms of Cartesian position and velocity. These vectors are propagated according to the two-body non-linear equations of motion. The other takes advantage of the fact that the equations of motion describe an orbital path which is a conic section, which, for earth-orbiting satellites, is always an ellipse. Satellite motion can then be analyzed as a mean angular displacement along that elliptical path. The second method is used here because of the linear nature of the mean angular motion and its clarity of physical significance.

#### A. KEPLER TWO-BODY DYNAMICS

The orbital path is described as an ellipse of fixed shape and size located in a plane of fixed orientation with respect to the earth's inertial reference frame. The quantities describing this path, the classical orbital elements [1], consist of five constants and one time-dependent quantity. Two of the constants ( $a$ ,  $e$ ) describe size and shape of the orbit, while the other three ( $i$ ,  $\Omega$ ,  $\omega$ ) orient the orbital plane in space. The time-dependent quantity ( $v$ ) pinpoints the actual location of the satellite on the orbital path. These elements are (see fig. 3.1):

- $a$  (semi-major axis) - defines size of the elliptical orbit.
- $e$  (eccentricity) - defines shape (non circularity) of orbit.

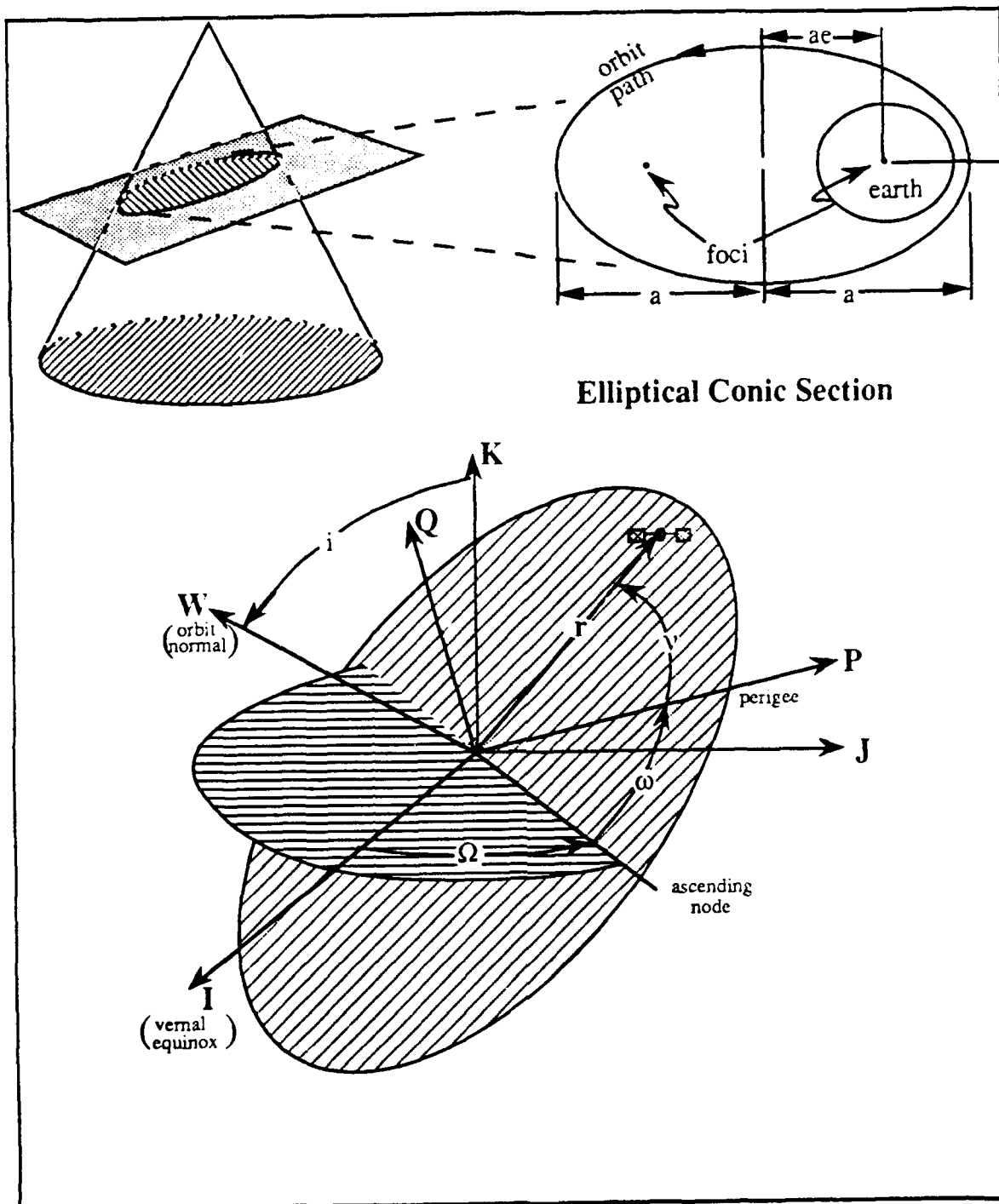


Figure 3.1. Classical orbital elements.

i (inclination) - defines the angle between equatorial plane normal (**K**) and orbital plane normal (**W**).

$\Omega$  (longitude of the ascending node) - defines the angle between the vernal equinox direction (**I**) and the point where the satellite crosses the equatorial plane from southern to northern hemisphere (ascending node).

$\omega$  (argument of perigee) - defines the angle between the ascending node and the satellite's closest point of approach (perigee).

v (true anomaly) - defines the angle between perigee and the satellite's actual position.

The elliptical orbital path, is described by the equation of a conic section

$$r = \frac{a(1 - e^2)}{1 + e \cos v} \quad (3.1)$$

where r is the magnitude of the satellite's position vector at a specified v. In general, v is nonlinear with respect to time, so the mean anomaly M, which varies linearly with respect to time for purely Keplerian motion, will be used as a filter state instead. M is related to v through a quantity called eccentric anomaly E. It is defined as follows (see fig. 3.2):

$$M = E - e \sin E \quad (3.2)$$

$$\cos v = \frac{\cos E - e}{1 - e \cos E} \quad (3.3)$$

$$\sin v = \frac{\sin E \sqrt{1 - e^2}}{1 - e \cos E} \quad (3.4)$$

Eqs. 3.1-3.4 define the relationship between  $M$  and  $r$ .

The filter state vector will be

$$\mathbf{x}_k = [a_k \quad e_k \quad i_k \quad \Omega_k \quad \omega_k \quad M_k]^T \quad (3.5)$$

where

$$\begin{bmatrix} a_{k+1} \\ e_{k+1} \\ i_{k+1} \\ \Omega_{k+1} \\ \omega_{k+1} \\ M_{k+1} \end{bmatrix} = \begin{bmatrix} a_k \\ e_k \\ i_k \\ \Omega_k \\ \omega_k \\ a_k^{-3/2} T_k + M_k \end{bmatrix} = f(\mathbf{x}_k, T_k) \quad (3.6)$$

and  $T_k$  is the time between observations. For the classical 2-body case, it can be seen from eq. 3.6 that state propagation is a linear problem.

In order to improve the estimate of the state vector using available observations, it becomes necessary to compare the states with the observables in a common reference frame. Satellite position, which is implicitly a function of the states through the relationship in eqs. 3.1-3.4, can be written

$$\mathbf{r}^P = \begin{bmatrix} r \cos v \\ r \sin v \\ 0 \end{bmatrix} \quad (3.7)$$

where  $\mathbf{r}^P$  denotes a position vector in the orbital (**PQW**) reference frame (see fig. 3.1). The remaining states are used to transform satellite position from orbital to inertial (**IJK**) coordinates using

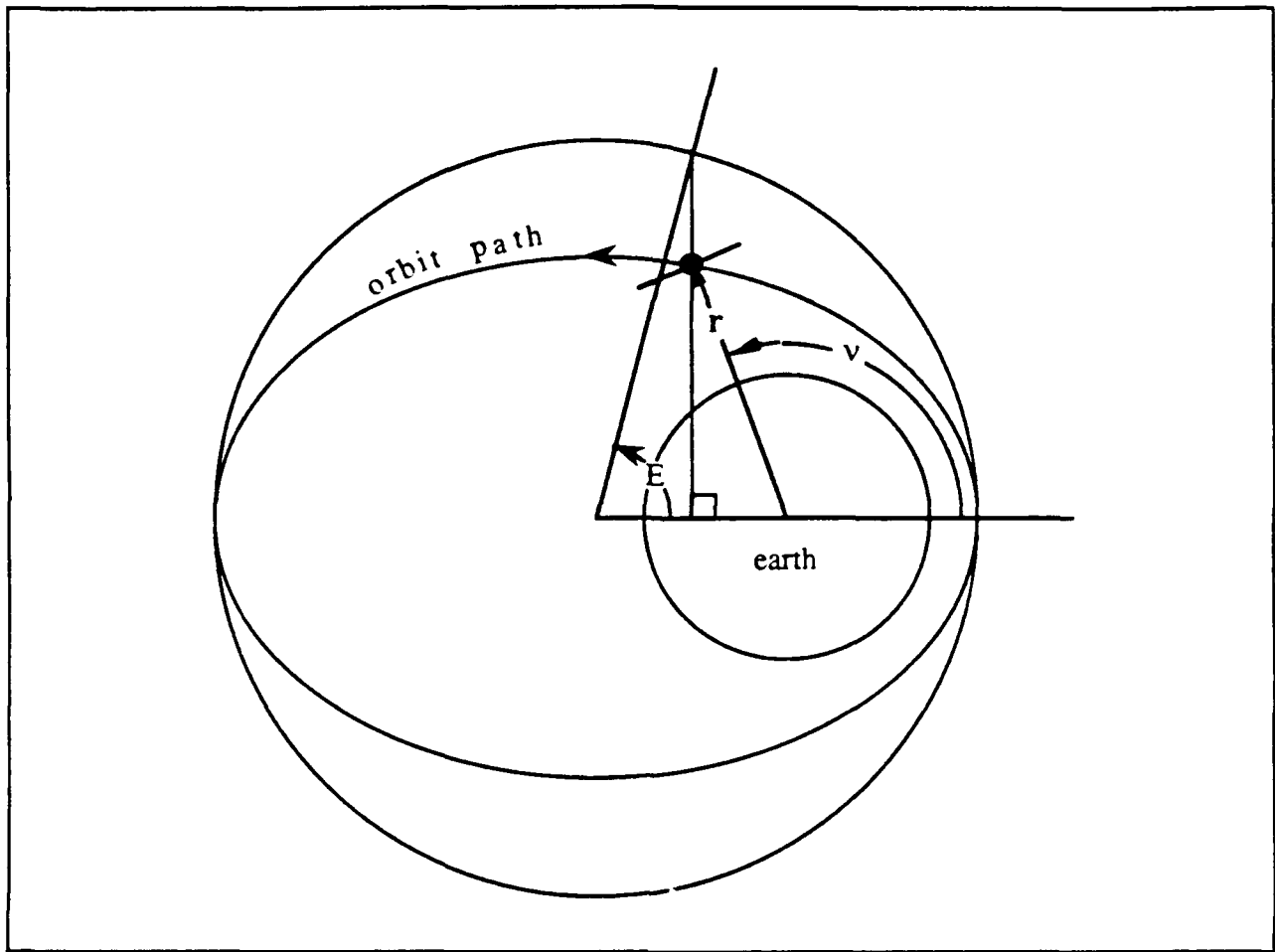


Figure 3.2. Eccentric vs. true anomaly.

$$C^{\frac{1}{2}} = \begin{bmatrix} c\omega c\Omega - s\omega s\Omega ci & -s\omega c\Omega - c\omega s\Omega ci & s\Omega si \\ c\omega s\Omega + s\omega c\Omega ci & -s\omega s\Omega + c\omega c\Omega ci & -c\Omega si \\ s\omega si & c\omega si & ci \end{bmatrix} \quad (3.8)$$

where  $c\theta = \cos \theta$  and  $s\theta = \sin \theta$  for brevity. (See App. A for development of  $C^{\frac{1}{2}}$ .)

Then satellite position in inertial coordinates will be

$$\mathbf{r}^I = \mathbf{C}^* \begin{bmatrix} r \cos v \\ r \sin v \\ 0 \end{bmatrix} \quad (3.9)$$

Now, inertial satellite coordinates need to be related to a measurement in the site-based reference frame.

## B. OBSERVATIONS

The detection scheme modeled here is a fixed planar radar beam generated by multiple continuous wave transmitters along a great circle path (see fig. 3.3). As a satellite penetrates this beam, phase information is collected at one or more of the receivers. Antenna geometry at each site makes it possible to compute direction cosines, which are the pseudo-observations available for element set improvement. These observables are (see fig. 3.4)

$$\cos \alpha = \frac{\bar{\rho} \cdot \mathbf{E}}{|\bar{\rho}|} \quad (3.10)$$

$$\cos \beta = \frac{\bar{\rho} \cdot \mathbf{N}}{|\bar{\rho}|}$$

where East-West cosine =  $\cos \alpha$  and North-South cosine =  $\cos \beta$ . ( $\gamma$  can be calculated from:  $\cos^2 \gamma + \cos^2 \beta + \cos^2 \alpha = 1$ .)

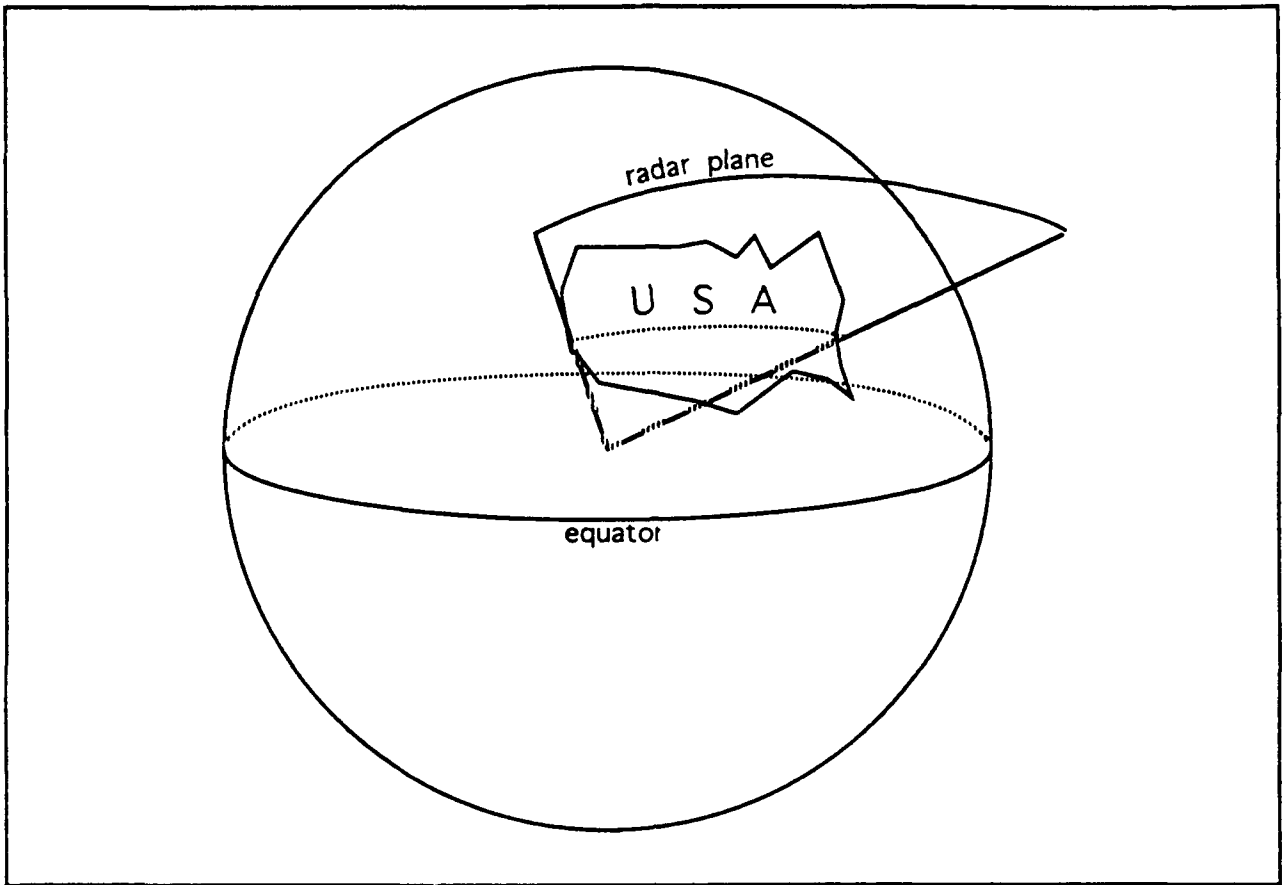


**Figure 3.3. Radar plane geometry.**

We have

$$\rho \cos \alpha = \bar{\rho} \cdot \mathbf{E} \quad (3.11)$$

$$\rho \cos \beta = \bar{\rho} \cdot \mathbf{N}$$

and

$$\hat{\mathbf{z}} = \begin{bmatrix} \cos \alpha \\ \cos \beta \end{bmatrix} \quad (3.12)$$

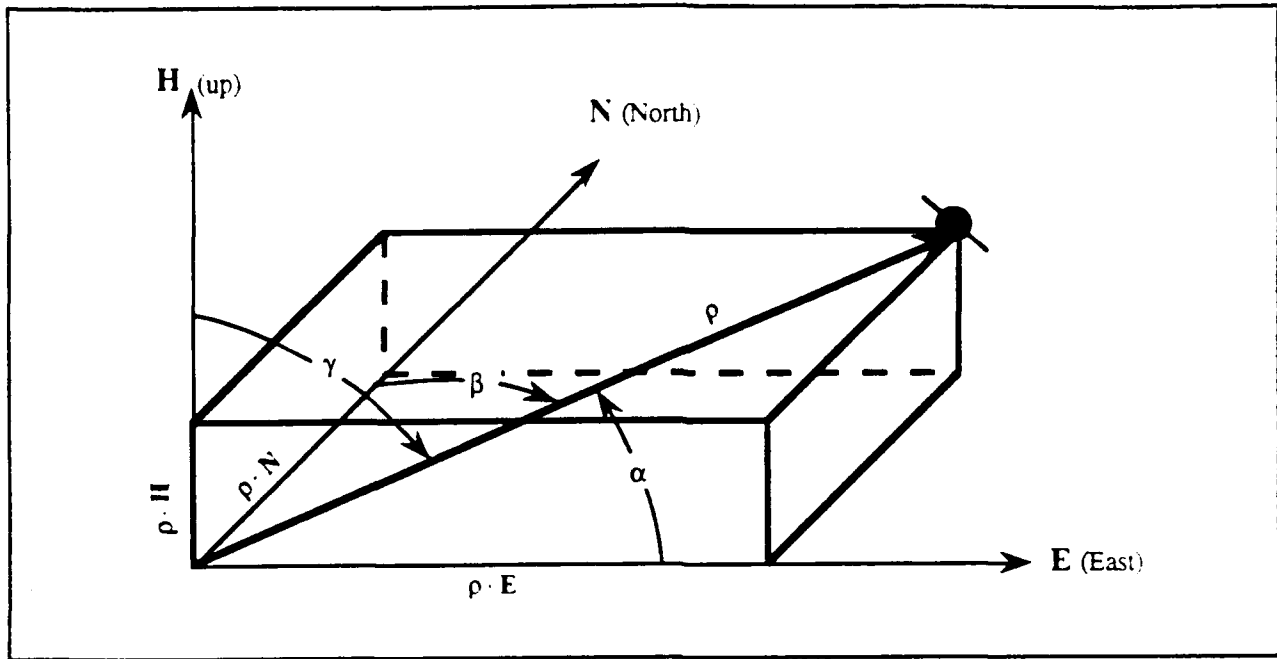


Figure 3.4. Receiver site geometry.

is the vector of observables to be used for orbital parameter improvement. (See App. B for development of  $\hat{z}$  in terms of the orbital elements.)

The position vector in the site-based frame is

$$\mathbf{r}^H = \mathbf{C}^H \mathbf{r}^I \quad (3.13)$$

where

$$\mathbf{C}^H = \begin{bmatrix} c\ell c\phi & c\ell s\phi & s\ell \\ -s\phi c(az) - s\ell c\phi s(az) & c(az)c\phi - s(az)s\ell s\phi & s(az)c\ell \\ s(az)s\phi - c(az)s\ell c\phi & -s(az)c\phi - c(az)s\ell s\phi & c(az)c\ell \end{bmatrix} \quad (3.14)$$

and

$\ell$  = latitude of receiver

$\phi = \omega_{\oplus}(t - t_0) - \text{lon}_{\text{site}}$

$\omega_{\oplus}$  = earth's rotation rate

$t_0$  = time of last Greenwich crossing of vernal equinox

$\text{lon}_{\text{site}}$  = longitude of receiver

(See fig. 3.5)

(See App. A for development of  $C^{\frac{H}{I}}$ ).

Recapitulating,

$$\mathbf{x}_k = f(\mathbf{x}_{k-1}, T_{k-1})$$

$$\mathbf{z}_k = g(\mathbf{x}_k, T_k) \quad (3.15)$$

both of which are, in general, nonlinear functions of the orbital elements  $\mathbf{x}_k$ . Assuming for now that perturbations to the two body dynamics and observation noise can be modeled as additive zero mean, white noise processes, the state and measurement equations become

$$\mathbf{x}_k = f(\mathbf{x}_{k-1}, T_{k-1}) + \mathbf{w}_{k-1} \quad (3.16)$$

$$\mathbf{z}_k = g(\mathbf{x}_k, T_k) + \mathbf{v}_k$$

Kalman filter equations are then

$$\hat{\mathbf{x}}_{k|k-1} = f(\hat{\mathbf{x}}_{k-1|k-1}, T_{k-1})$$

$$\mathbf{P}_{k|k-1} = \hat{\Phi} \mathbf{P}_{k-1|k-1} \hat{\Phi}^T + \mathbf{Q}$$

$$\mathbf{G}_k = \mathbf{P}_{k|k-1} \hat{\mathbf{H}}^T [\hat{\mathbf{H}} \mathbf{P}_{k|k-1} \hat{\mathbf{H}}^T + \mathbf{R}]^{-1}$$

$$\begin{aligned}\hat{\mathbf{x}}_{k/k} &= \hat{\mathbf{x}}_{k/k-1} + \mathbf{G}_k (\mathbf{z}_k - \hat{\mathbf{z}}_{k/k-1}) \\ \mathbf{P}_{k/k} &= (\mathbf{I} - \mathbf{G}_k \hat{\mathbf{H}}) \mathbf{P}_{k/k-1}\end{aligned}\quad (3.17)$$

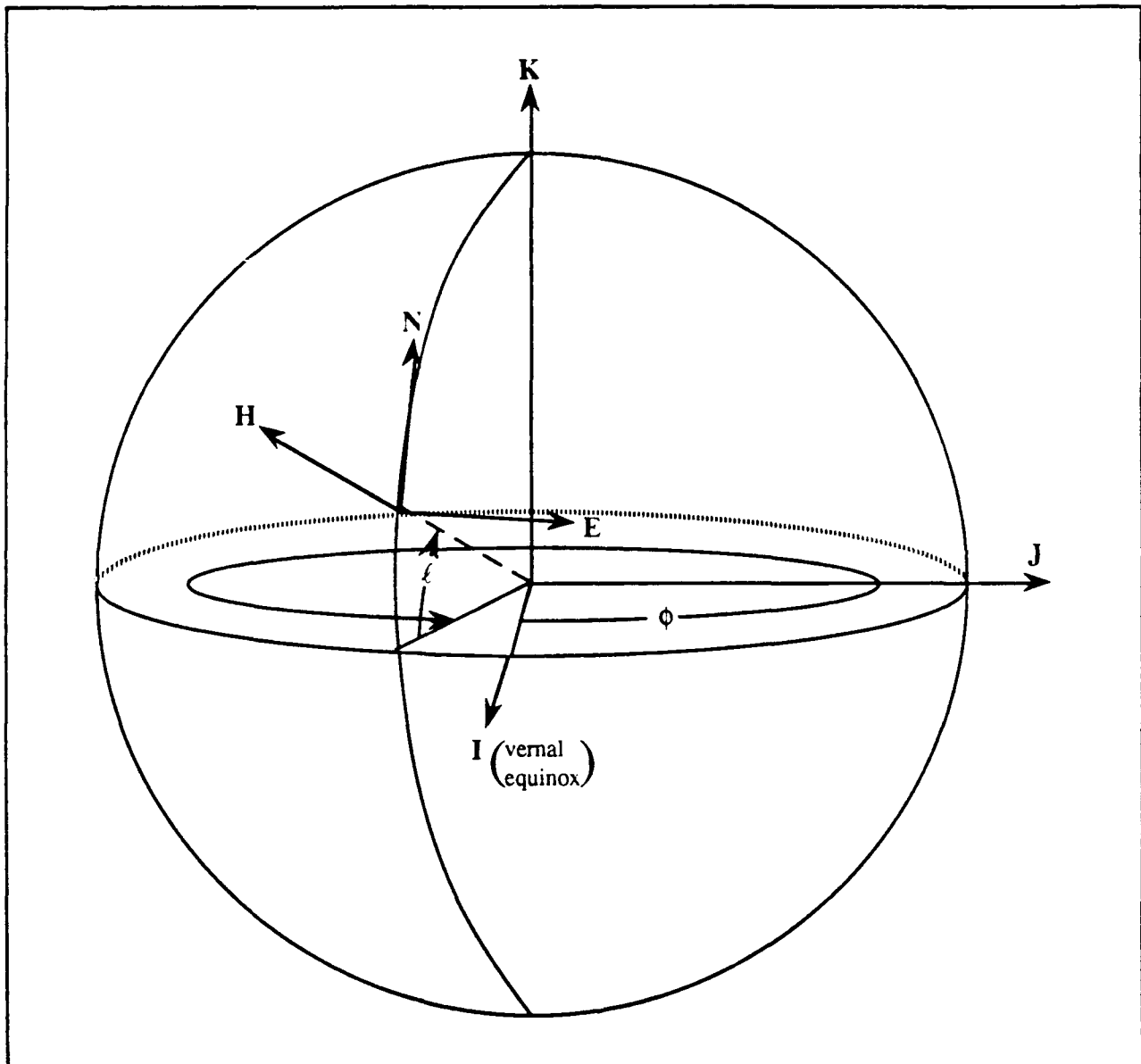


Figure 3.5. Receiver site geometry.

where

$$\mathbf{Q} = \mathbf{E}[\mathbf{w}_k \mathbf{w}_k^T]$$

$$\mathbf{R} = \mathbf{E}[\mathbf{v}_k \mathbf{v}_k^T]$$

$$\mathbf{P}_k = \mathbf{E}\left[\left(\hat{\mathbf{x}}_{k/k} - \mathbf{x}_k\right)\left(\hat{\mathbf{x}}_{k/k} - \mathbf{x}_k\right)^T\right]$$

$$\hat{\Phi} = \left. \frac{\partial f(\mathbf{x}_k, T_k)}{\partial \mathbf{x}_k} \right|_{\hat{\mathbf{x}}_{k-1}, T_{k-1}}$$

$$\hat{\mathbf{H}} = \left. \frac{\partial g(\mathbf{x}_k, T_k)}{\partial \mathbf{x}_k} \right|_{\hat{\mathbf{x}}_{k-1}, T_{k-1}}$$

$$\hat{\mathbf{z}}_{k-1} = g(\mathbf{x}_{k-1}, T_{k-1}) \quad (3.18)$$

$$\mathbf{z}_k = \begin{bmatrix} \rho \cos \alpha \\ \rho \cos \beta \end{bmatrix}_k$$

(See App. B for derivations of  $\hat{\Phi}$  and  $\hat{\mathbf{H}}$ .)

In words, the actual observations,  $\mathbf{z}_k$ , are compared with computed observations,  $\hat{\mathbf{z}}_{k-1}$  (based on the classical two-body propagation model), resulting in the Kalman filter innovations. These are multiplied by the filter gain, which is based on the dynamic model and measurement uncertainties and used to produce an improved estimate of the orbital elements.

### C. RADAR PLANE INTERSECTION

Meaningful application of the observations to orbital element set improvement requires the ability to predict subsequent penetrations of the radar plane by the satellite in question. A simple way to do this is to define the satellite's position vector in a coordinate frame referenced to the radar plane (See fig. 3.6). Then the out of plane component (**Z**) of position can be checked for a value of zero, yielding an in-plane condition.

Satellite position, readily available in orbital frame coordinates ( $\mathbf{r}^P$ ) is transformed to radar plane coordinates by performing two coordinate transformations: one from orbital to inertial frame, the other from inertial to radar plane frame, or

$$\mathbf{r}^X = \mathbf{C}^{XI} \mathbf{C}^{IP} \mathbf{r}^P \quad (3.19)$$

where  $\mathbf{r}^X$  denotes a position vector in the radar plane (**XYZ**) reference frame and

$$\mathbf{C}^{XI} = \begin{bmatrix} c\theta_{\pi} c\theta & c\theta_{\pi} s\theta & s\theta_{\pi} \\ -s\theta & c\theta & 0 \\ -s\theta_{\pi} c\theta & -s\theta_{\pi} s\theta & c\theta_{\pi} \end{bmatrix} \quad (3.20)$$

where

$$\theta = \omega_{\oplus} (t - t_0) - \text{lon}_x,$$

$\theta_{\pi}$  is the inclination of the radar plane to the equatorial plane

$\text{lon}_r$  is the longitude where the maximum latitude of the radar plane occurs, which describes the location of the X-axis of the radar plane reference frame. (See fig. 3.6).

(See App. A for development of  $C^{\text{X}}_r$ .)

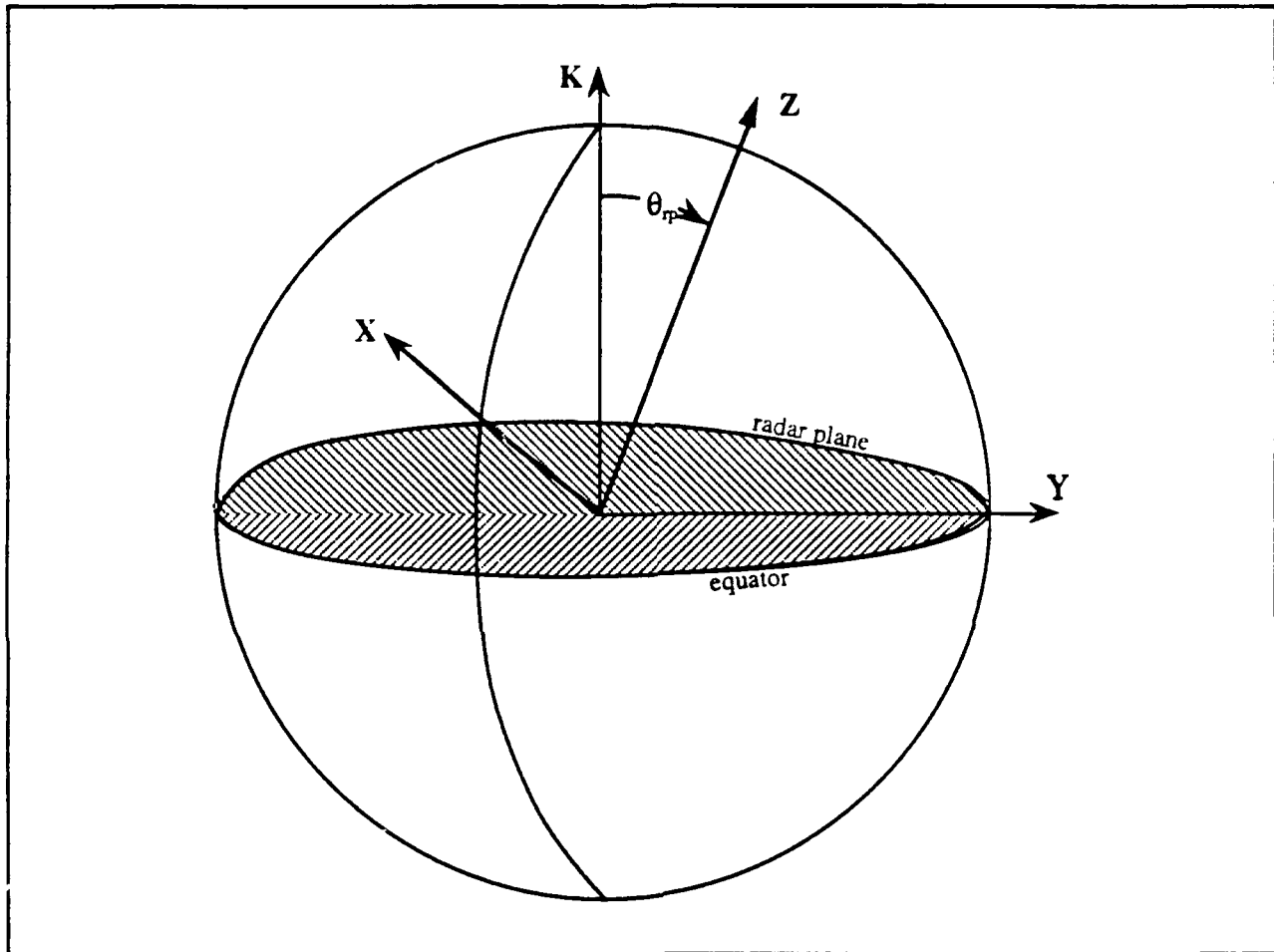


**Figure 3.6. Radar plane orientation.**

Since the only component of satellite position of interest in determining radar plane intersection is the **Z**-component, the expression can be further simplified to

$$\begin{aligned}
r_z &= [0 \quad 0 \quad 1] C^X C^Y P \\
&= [-s\theta_{\pi} P_1 c\theta - s\theta_{\pi} P_4 s\theta + c\theta_{\pi} P_7] r \cos v \\
&\quad + [-s\theta_{\pi} P_2 c\theta - s\theta_{\pi} P_5 s\theta + c\theta_{\pi} P_8] r \sin v
\end{aligned} \tag{3.21}$$

where

$$C^Y = \begin{bmatrix} P_1 & P_2 & P_3 \\ P_4 & P_5 & P_6 \\ P_7 & P_8 & P_9 \end{bmatrix} \tag{3.22}$$

The in-plane condition of relevance to the filter is that which falls inside the field of view of one of multiple receiver sites, also placed along the great circle path circumscribed by the transmitters. The time epoch of this condition is the time close to which we expect to observe the satellite from one or more of the radar plane receivers.

## IV. DOMINANT PERTURBATIONS

Satellite orbital parameters deviate from Keplerian motion deterministically and randomly due to many factors. Ignoring for now such intentional human-caused phenomenon as plane change and stationkeeping maneuvers, the largest natural contributor to parameter variations is the nonuniformity of the gravitational field due to earth's oblateness. For low earth orbits, the next most significant factor is atmospheric drag.

### A. GRAVITY PERTURBATIONS

The largest contributor to perturbations to the Keplerian orbital elements arises from the oblateness of the earth. These perturbations take the form of a combination of secular and periodic variations of the classical orbital elements. Many solutions have been developed for this problem, each with its own strengths and weaknesses. All the solutions, however, are based on the gravitational potential

$$U = \frac{\mu_{\oplus}}{r} \left\{ 1 - \sum_{n=2}^{\infty} \frac{1}{r^n} J_n P_n(\sin \delta) \right\} \quad (4.1)$$

where

$\mu_{\oplus}$  is earth's gravitational parameter

$r$  is the distance of the satellite from earth's center

$J_n$  are  $n^{\text{th}}$  order zonal harmonics

$P_n(\sin \delta)$  are Legendre polynomials

$\delta$  is satellite declination

and are more or less complex depending on the order to which the terms of the expression are carried. This expression for  $U$  already carries with it a degree of simplification in that it assumes axial symmetry for the earth. In truth, the equator is slightly elliptical, but the main effect is on the stability of geosynchronous satellites, since their orbits are in the equatorial plane [3]. Further simplification is accomplished by dropping terms for  $n \geq 3$ . This is justified for medium accuracy applications because of relative magnitudes of the  $J_n$  terms

$$\begin{aligned} J_2 &= 1.0826 \cdot 10^{-3} \\ J_3 &\approx -2 \cdot 10^{-6} \\ J_5 &\approx -2 \cdot 10^{-7} \\ &\vdots \end{aligned} \tag{4.2}$$

where  $J_n$  successively decrease. So the simplified potential function is

$$U = -\left( \frac{\mu_{\oplus}}{r} + \frac{\mu_{\oplus}}{r^3} J_2 (3 \sin^2 \delta - 1) \right) \tag{4.3}$$

Defining  $R = \frac{\mu_{\oplus}}{r^3} J_2 (3 \sin^2 \delta - 1)$  as the perturbing function, the variation of that function with respect to each of the orbital elements is [ 4 ]

$$\begin{aligned}
\frac{\partial R}{\partial a} &= -\frac{3}{a} R \\
\frac{\partial R}{\partial e} &= \frac{3J_2}{2(1-e^2)r^3} \left[ \cos \omega (1+e \cos v) (1-3 \sin^2 i \cdot \sin^2 u) \right. \\
&\quad \left. - \sin^2 i \cdot \sin 2u \cdot \sin v (2+e \cos v) \right] \\
\frac{\partial R}{\partial i} &= \frac{-3J_2}{r^3} \sin i \cdot \cos i \cdot \sin^2 u \\
\frac{\partial R}{\partial \omega} &= \frac{-3J_2}{2r^3} \sin^2 i \cdot \sin 2u \\
\frac{\partial R}{\partial \Omega} &= 0 \\
\frac{\partial R}{\partial M} &= \frac{1}{n} \frac{dR}{dt}
\end{aligned} \tag{4.4}$$

To develop a first order theory, the right-hand members of eq. 4.4 are expanded in a Taylor series about the initial orbital element values, retaining only the first term of the expansion, yielding expressions for the derivative of each orbital element with respect to true anomaly  $v$ . Integrating these expressions yields an analytical first order solution in the form

$$\mathbf{x} = \mathbf{x}_0 + \delta_s \mathbf{x}(v) + \delta_p \mathbf{x}(v) \tag{4.5}$$

where

$\mathbf{x}$  = instantaneous orbital elements

$\mathbf{x}_0$  = initial orbital elements

$\delta_s \mathbf{x}$  = secular variations as a function of  $v$

$\delta_p \mathbf{x}$  = periodic variations as a function of  $v$

All six orbital elements experience periodic variations. However, only  $\Omega$ ,  $\omega$  and  $M$  experience secular perturbations. These are

$$\begin{aligned}\delta_t \Omega &= -\frac{3J_2}{4p^2} [\cos i_o] 2(v - v_o) \\ \delta_t \omega &= \frac{3J_2}{2p^2} \left[ 2 - \frac{5}{2} \sin^2 i_o \right] (v - v_o) \\ \delta_t M &= n_o \left[ 1 + \frac{J_2}{a_o^2} \left( \frac{a_o}{r_o} \right)^3 (1 - 3 \sin^2 \delta_o) \right]^{\frac{3}{2}} (t - t_o)\end{aligned}\tag{4.6}$$

Note that  $\delta_t M$  is expressed in terms of independent variable  $t$ , which is the time at which true anomaly is equal to the value of  $v$  in  $\delta_t \Omega$  and  $\delta_t \omega$ . The periodic variations in  $\omega$  and  $M$  do carry  $1/e_o$  terms which approach singularity for near circular orbits. This can be explained by the fact that  $\omega$  and  $M$  are undefined for circular orbits and ill-defined for near circular orbits. Fortunately, the combination of  $\omega + M$  obviates the singular condition by effectively forming one new orbital element out of  $\omega$  and  $M$ .

Long term propagation of the orbital elements, assuming a drag-free environment, is accomplished by applying only the secular variations, since periodic variations will have no net effect on the elements over time. However, the periodic variations will be seen later to come into play when observations are assimilated into the orbital element improvement process. Inclusion of these secular variations in the dynamic model yields

$$\mathbf{x}_{k+1} = f(\mathbf{x}_k, T_k) \quad (4.7)$$

where

$$f(\mathbf{x}_k, T_k) = \begin{bmatrix} a_k \\ e_k \\ i_k \\ \Omega_k - \frac{3J_2}{2p_k^2} [\cos(i_k)](v_{k+1} - v_k) \\ \omega_k + \frac{3J_2}{2p_k^2} \left[ 2 - \frac{5}{2} \sin^2 i_k \right] (v_{k+1} - v_k) \\ M_k + n_k \left[ 1 + \frac{J_2}{a_k^2} \left( \frac{a_k}{r_k} \right)^3 (1 - 3 \sin^2 \delta_k) \right]^{\frac{3}{2}} T_k \end{bmatrix} \quad (4.8)$$

where

$p_k = a_k (1 - e_k^2)$  is the semi-latus rectum of the orbit

$J_2$  is the second order zonal harmonic (equatorial bulge).

The gravitational force model which gives rise to these secular variations is relatively simple. It assumes that the earth is symmetric about its spin axis and about the equatorial plane. Noteworthily, the first three mean orbital elements experience no secular variation due to earth's oblateness.

It may be possible to maintain identification of some satellites using secular variations alone. Continuous identification of a satellite, however, may depend upon the application of the periodic variations to the mean elements at observation times. These periodic variations are assimilated as an additive (superposition assumed) adjunct to the existing dynamic model and therefore are not technically a part of the propagation dynamics. The filter innovations resulting from a comparison of observables with predicted states are then applied, via the Kalman gains, to the mean elements, implying a prior removal of the periodic variations. These periodic variations, to first order, and ignoring terms of the order of  $e_0$  and smaller, are

$$\begin{aligned}
\delta a_p &= \frac{3J_2 a_0}{2p_0^2(1-e_0^2)} \sin^2 i_0 \cdot \cos[2(\omega_0 + v)] \\
\delta e_p &= \frac{3J_2}{2p_0^2} \left[ \left(1 - \frac{3}{2} \sin^2 i_0\right) \cos v + \frac{1}{4} \sin^2 i_0 \cdot \cos(2\omega_0 + v) \right. \\
&\quad \left. + \frac{7}{12} \sin^2 i_0 \cdot \cos(2\omega_0 + 3v) \right] \\
\delta i_p &= -\frac{3J_2}{8p_0^2} \sin(2i_0) \cos[2(\omega_0 + v)] \\
\delta \Omega_p &= \frac{3J_2}{4p_0^2} \cos i_0 \cdot \sin[2(\omega_0 + v)] \\
\delta \Omega_p &= \frac{3J_2}{4p_0^2} \cos i_0 \cdot \sin[2(\omega_0 + v)] \\
\delta M_p &= -\frac{3J_2}{4p_0^2} \left(1 - \frac{5}{2} \sin^2 i_0\right) \sin[2(\omega_0 + v)]
\end{aligned} \tag{4.9}$$

## B. DRAG PERTURBATIONS

Satellites traveling in the altitude regime below 600 km experience non-negligible drag force due to atmospheric resistance [3]. This force is well represented as

$$F_D = \frac{1}{2} C_D \frac{A}{m} \rho V^2 \quad (4.10)$$

where

$m$ =mass of satellite

$C_D \approx 2$  is a dimensionless drag coefficient

$A$ = effective cross sectional area of satellite

$V$ = velocity of satellite with respect to atmosphere

$\rho$ =local atmospheric density.

### 1. Atmospheric Drag Effects

To first order, drag force doesn't affect  $i$  and  $\Omega$  [6]. The main effects of this drag force are to bring about secular decreases in  $a$  and  $e$ , i.e., to decrease the size and eccentricity of the orbit.  $\omega$  and  $M$  also experience changes due to drag, but these are negligible compared to the oblateness effects.

It turns out that

$$\frac{da}{dM} = -\frac{C_D A}{m} \rho a^2 \left( \frac{1+e \cos E}{1-e \cos E} \right)^{\frac{3}{2}} (1-\tau)^2 \quad (4.11)$$

where

$$\tau = \frac{d(1 - e \cos E)}{1 + e \cos E}$$

$$d = \frac{\omega_e}{n} (1 - e^2)^{1/2} \cos i \quad (4.12)$$

$$n = \sqrt{\frac{\mu}{a^3}}$$

and

$$\begin{aligned} \frac{de}{dM} = & -\frac{C_D A}{m} \rho a (1 - e^2) \frac{(1 + e \cos E)^{1/2}}{(1 - e \cos E)^{3/2}} (1 - \tau)^2 \cos E \\ & - \frac{C_D A}{2m} \rho a e d \left( \frac{1 - e \cos E}{1 + e \cos E} \right)^{1/2} (1 - \tau) \sin^2 E \end{aligned} \quad (4.13)$$

All quantities in these two expressions are well known (according to the simplified model) except for atmospheric density  $\rho$ , the value of which is related to space and time in a complex manner. Atmospheric models delivering as good as 15% standard deviation are in the form of tables or very complicated empirical formulae or both [13]. For simplicity, it is advantageous to use an analytical function to model  $\rho$ . It is assumed that variations in  $\rho$  in the upper atmosphere (150 km to 750 km) are a superposition of four individual variations [4].

The first variation is diurnal, or, daily. This fluctuation has to do with change in solar flux intensity associated with moving from darkness to daylight, and vice versa. Density, depending on latitude and altitude, may change by up to a factor of 10.

The second type is related to the 11 year solar cycle which is motivated by intensity of sunspot activity. Maximum density, occurring at the peak of sunspot activity, is roughly ten times the mean density.

A third variation is semiannual, with density falling to a minimum in July and a maximum in October, with a less pronounced minimum and maximum in January and April, respectively. The range of this variation is, generally, less than 1/20 the range of the 11 year solar cycle.

The fourth type of variation is nonperiodic and unpredictable and is tied to geomagnetic storms rising from solar flare eruptions. Atmospheric density may increase by a factor of 10 from the geomagnetic quiescent value.

Over the short term (days), barring magnetic storms, the diurnal variation dominates. However, over several years, the solar cycle has a more profound effect on atmospheric density.

The modeling approach followed here was to start with a very simple, even crude, atmospheric density model, including the above considerations as necessary to achieve desired accuracy.

## 2. Simplified Drag Effects

First, simpler expressions for changes in  $a$  and  $e$  due to drag can be developed by viewing these changes as a result of orbital specific energy being extracted by drag force [14]. Specific energy of an orbit, which is conserved for an unperturbed Keplerian orbit, can be expressed as

$$\epsilon = \frac{1}{2} V^2 - \frac{\mu}{r} = -\frac{\mu}{2a} \quad (4.14)$$

The change in  $a$  for an incremental change in  $\epsilon$  is then

$$da = \frac{2a^2}{\mu} d\epsilon \quad (4.15)$$

If it is assumed that most of the drag occurs near perigee (atmospheric density exponentially decreasing with altitude), then

$$r = r_p = a(1 - e) \quad (4.16)$$

from eq. 3.1, and

$$\begin{aligned} V^2 r &= \mu \left( 2 - \frac{r}{a} \right) \\ &= \mu(1 + e) \end{aligned} \quad (4.17)$$

from eqs. 4.13 and 4.15. For a satellite moving through  $dv$  near perigee (see fig. 4.1), the specific energy extracted will be

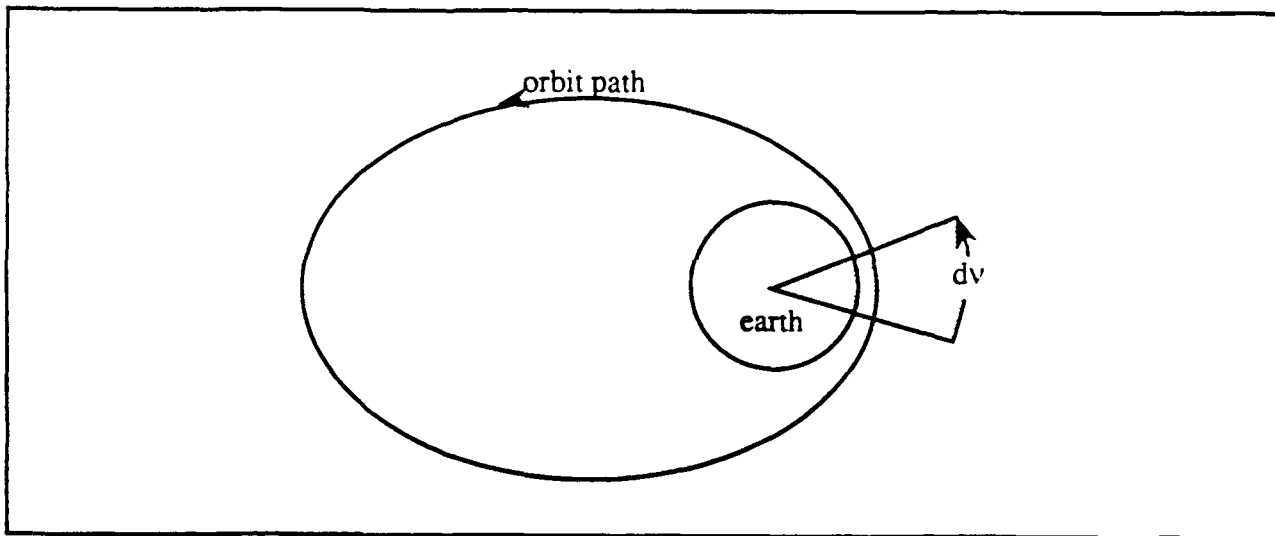


**Figure 4.1. Satellite moving through perigee.**

$$\begin{aligned}
d\epsilon &= -\frac{F_D}{m} r dv \\
&= -\frac{1}{2} \left( \frac{C_D A}{m} \right) \rho V^2 r dv
\end{aligned} \tag{4.18}$$

Substituting eq. 4.17 into eq. 4.18 yields

$$d\epsilon = -\frac{1}{2} \left( \frac{C_D A}{m} \right) \rho \mu (1+e) dv \tag{4.19}$$

Substituting eq. 4.19 into eq. 4.15 gives an expression for decrease in semi-major axis due to a decrease in orbital energy

$$da = -\left( \frac{C_D A}{m} \right) a^2 (1+e) \rho dv \tag{4.20}$$

Since the new orbit will pass through the same perigee point, all of  $da$  shows up as a decrease in apogee radius, and

$$dr_p = da(1-e) - ade = 0 \tag{4.21}$$

by differentiating eq. 4.16. Solving for  $de$  gives

$$de = \frac{da}{a} (1-e) = -\left( \frac{C_D A}{m} \right) a (1-e^2) \rho dv \tag{4.22}$$

### 3. Atmospheric Drag Characterization

A crude model for variation of  $\rho$  starts with the assumption that temperature and chemical composition of a gas remain constant [14]. Then, density is directly proportional to pressure according to

$$\rho = kP \quad (4.23)$$

(Realistically,  $k$  is a function of temperature and chemical composition.) At an altitude  $h$ , the decrease in pressure accompanying an increase in altitude is

$$dP = -\rho g dh \quad (4.24)$$

where  $g$  is acceleration of gravity. Since  $k$  is assumed constant,

$$dP = \frac{1}{k} d\rho \quad (4.25)$$

Combining eqs 4.24 and 4.25 yields

$$\frac{d\rho}{\rho} = -kg dh$$

$$\int_{\rho_0}^{\rho} \frac{d\rho}{\rho} = -kg \int_0^h dh \quad (4.26)$$

$$\rho = \rho_0 e^{-kg h}$$

So, in general, atmospheric density decreases exponentially with altitude.

Eq. 4.26 can be rewritten

$$\rho = \rho_0 e^{-h/h_0} \quad (4.27)$$

where  $\rho_0$  (reference air density) and  $h_0$  (density scale height) change for different altitude regimes. For example, using standard fixed values of  $\rho$  from the "U.S.

Standard Atmosphere, 1976," a reasonable fit can be made by applying the values in Table 4.1 for the ranges of altitude shown.

**Table 4.1. DRAG PARAMETERS.**

Altitude	$\rho_0$ (kg/m <sup>3</sup> )	$z_0$ (km)
80 km<z<120 km	18.5	5.8
120 km<z<140 km	$1.21 \times 10^{-3}$	11
140 km<z<200 km	$3.00 \times 10^{-6}$	21

## **V. THE RECURSIVE ORBITAL PARAMETER ESTIMATOR**

An extended Kalman filter, designed for orbital parameter estimation, is based on the earth-fixed radar plane detection scenario described in Chap. III (Also see fig. 5.1). The filter propagates the orbital elements in time according to a first order nonlinear dynamic model which takes into account the dominant perturbations arising from earth oblateness and atmospheric drag. Upon receiving observations, in the form of pairs of direction cosines, the filter calculates an improvement to the current parameter estimate. The filter operates recursively as observations become available. The filter is written in Matlab code and can be found in App. C.

### **A. FILTER INITIALIZATION**

The estimator is designed to receive two data files. One contains an initial set of orbital elements along with subsequent pairs of available direction cosines (see App. C). The other holds information about the receiver sites. Values of pertinent constants are also set, as are the initial times necessary for orbit propagation and estimation of observables.

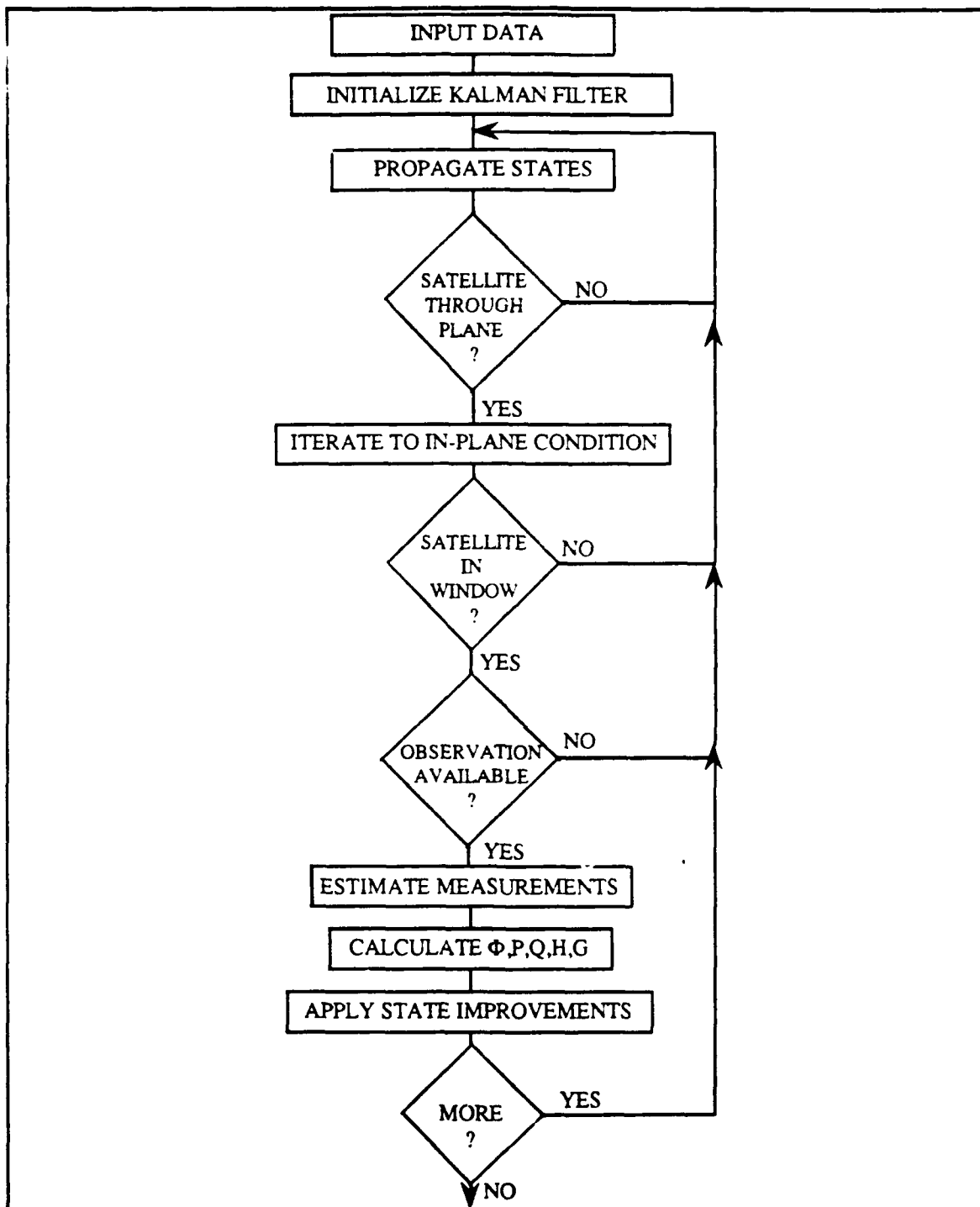


Figure 5.1. Estimator flow chart.

## 1. Input Data Files

Two input files are required for filter operation. One contains an initial set of orbital parameters, along with subsequent sets of direction cosines. This information is all tagged with corresponding times (see App. C). The last five orbital elements occur in classical orbital element form, but, in lieu of semi-major axis, orbital period is given. The conversion is simply

$$\begin{aligned} a &= \left( \frac{T_{\text{sat}} \mu_{\oplus}^{1/2}}{2\pi} \right)^{2/3} \\ &= \left( \frac{T_{\text{sat}}}{2\pi} \right)^{2/3} \end{aligned} \quad (5.1)$$

where  $T_{\text{sat}}$  is the period of the satellite. Note here the apparent disappearance of earth's gravitational parameter  $\mu_{\oplus}$ . This convenience is brought about by the use of canonical units [1], where

$$\mu_{\oplus} = 1 \frac{\text{DU}_{\oplus}^3}{\text{TU}_{\oplus}^2}$$

1  $\text{DU}_{\oplus} = 6378.135$  km and is earth's mean equatorial radius.

1  $\text{TU}_{\oplus} = 13.44686$  min and is the time it takes for a satellite traveling in a circular orbit at a radius of 1 DU to travel 1 DU of arc length.

Canonical units are used in all filter calculations. The other input file contains information on the receiver site locations, altitudes, and azimuths. The azimuthal measurement indicates, for each receiver, the angular offset of its coordinate frame from true north.

## 2. Constants

The earth's apparent rotation rate is initialized as

$$\omega_{\oplus} = .05883378 \text{ rad/TU} \quad (5.2)$$

The radar plane's inclination to the equatorial plane and the longitude of its center line are, respectively,

$$\begin{aligned} \theta_p &= 33.58310^\circ \\ \text{lon}_x &= -101.31348^\circ \end{aligned} \quad (5.3)$$

The radar plane is offset from earth's center by about 20 km, or

$$r_{\text{offset}} = .0031 \text{ DU}_{\oplus} \quad (5.4)$$

## 3. Time

All times are given in Universal Coordinated Time (UCT) and converted to  $\text{TU}_{\oplus}$ s for filter use.  $T_{\text{gmwch}}$ , which is time elapsed since the Greenwich meridian last passed the geocentric inertial **I** axis, is computed from a reference angle (measured from **I** to Greenwich) at 0 hrs, 1 Jan 92, of

$$\theta_{\text{gmwch}} = 98.920250931^\circ \quad (5.5)$$

using the  $\omega_{\oplus}$  given previously.

#### 4. Filter Matrices

The error covariance matrix  $\mathbf{P}$  is initialized to reflect the level of confidence placed in the accuracy of the initial orbital element set. The measurement error covariance matrix  $\mathbf{R}$  is set to

$$\mathbf{R} = \begin{bmatrix} \sigma_{\cos \alpha}^2 & 0 \\ 0 & \sigma_{\cos \beta}^2 \end{bmatrix} \quad (5.6)$$

where  $\sigma_{\cos \alpha} = \sigma_{\cos \beta} = .0002^\circ$  reflects the uncertainty of the available direction cosines.

#### B. STATE PROPAGATION

The filter states are propagated according to the two-body Keplerian orbital dynamics perturbed by earth oblateness and atmospheric drag. The nonlinear state equations are

$$f(\mathbf{x}_k, T_k) = \begin{bmatrix} a_k - \left( \frac{C_D A}{m} \right) a^2 (1+e) \rho (v_{k+1} - v_k) \\ e_k - \left( \frac{C_D A}{m} \right) a (1-e^2) \rho (v_{k+1} - v_k) \\ i_k \\ \Omega_k - \frac{3J_2}{2p_k^2} [\cos(i_k)] (v_{k+1} - v_k) \\ \omega_k + \frac{3J_2}{2p_k^2} \left[ 2 - \frac{5}{2} \sin^2 i_k \right] (v_{k+1} - v_k) \\ M_k + n_k \left[ 1 + \frac{J_2}{a_k^2} \left( \frac{a_k}{r_k} \right)^3 (1 - 3 \sin^2 \delta_k) \right]^{\frac{3}{2}} T_k \end{bmatrix} \quad (5.7)$$

and are propagated at arbitrary increments of  $T_{\text{m}}/8$ . This is continued until a crossing of the radar plane is detected by a sign change of the radar-plane-normal component of satellite position.

### C. RADAR PLANE INTERSECTION

Detection of a radar plane crossing calls a function which iterates to an in-plane condition for estimated satellite position. This is accomplished using a Newton-Rapson iteration on the expression for the plane-normal component of satellite position. The iteration calls for a calculation of an approximate  $\Delta M$  which will drive  $r_z$  to near zero. This is given by

$$\Delta M = \frac{-r_z}{\left(\partial r_z / \partial M\right)} \quad (5.8)$$

where, from eq. 3.21,

$$r_z = X_1 r \cos v + X_2 r \sin v \quad (5.9)$$

and

$$\begin{aligned} \frac{\partial r_z}{\partial M} = & \frac{\partial X_1}{\partial M} r \cos v + X_1 \frac{\partial(r \cos v)}{\partial M} \\ & + \frac{\partial X_2}{\partial M} r \sin v + X_2 \frac{\partial(r \sin v)}{\partial M} \end{aligned} \quad (5.10)$$

Taking the individual derivatives yields

$$\frac{\partial X_1}{\partial M} = -P_1 \sin \theta_{\pi} \frac{\partial(\cos \theta)}{\partial M} - P_4 \sin \theta_{\pi} \frac{\partial(\sin \theta)}{\partial M} \quad (5.11)$$

$$\frac{\partial X_2}{\partial M} = -P_2 \sin \theta_{\pi} \frac{\partial(\cos \theta)}{\partial M} - P_5 \sin \theta_{\pi} \frac{\partial(\sin \theta)}{\partial M}$$

where

$$\begin{aligned} \frac{\partial(\cos \theta)}{\partial M} &= -\omega_{\epsilon} a^{-3/2} (\sin \theta) \\ \frac{\partial(\sin \theta)}{\partial M} &= \omega_{\epsilon} a^{-3/2} (\cos \theta) \end{aligned} \quad (5.12)$$

and

$$\begin{aligned} \frac{\partial(r \cos v)}{\partial M} &= -\frac{a \sin E}{1 - e \cos E} \\ \frac{\partial(r \sin v)}{\partial M} &= -\frac{a \sqrt{1 - e^2} \cos E}{1 - e \cos E} \end{aligned} \quad (5.13)$$

where

$$\begin{aligned} r \cos v &= a(\cos E - e) \\ r \sin v &= a \sqrt{1 - e^2} \sin E \\ \frac{\partial E}{\partial M} &= \frac{1}{1 - e \cos E} \end{aligned} \quad (5.14)$$

This iteration is found to converge to within  $z, < \epsilon$  in three to four iterations, where  $\epsilon = 10^{-8}$ .

The function then determines whether the satellite is within the field of view of one or more receiver sites by calculating the in-plane  $r_x$  and  $r_y$  components of satellite position and checking the inequality (see fig. 5.2)

$$\frac{r_x}{\sqrt{r_x^2 + r_y^2}} \geq \cos 20^\circ \quad (5.15)$$

It should be noted here that the field of view needed to be opened up to pick up some satellite observations by receivers at the edges of the radar plane.

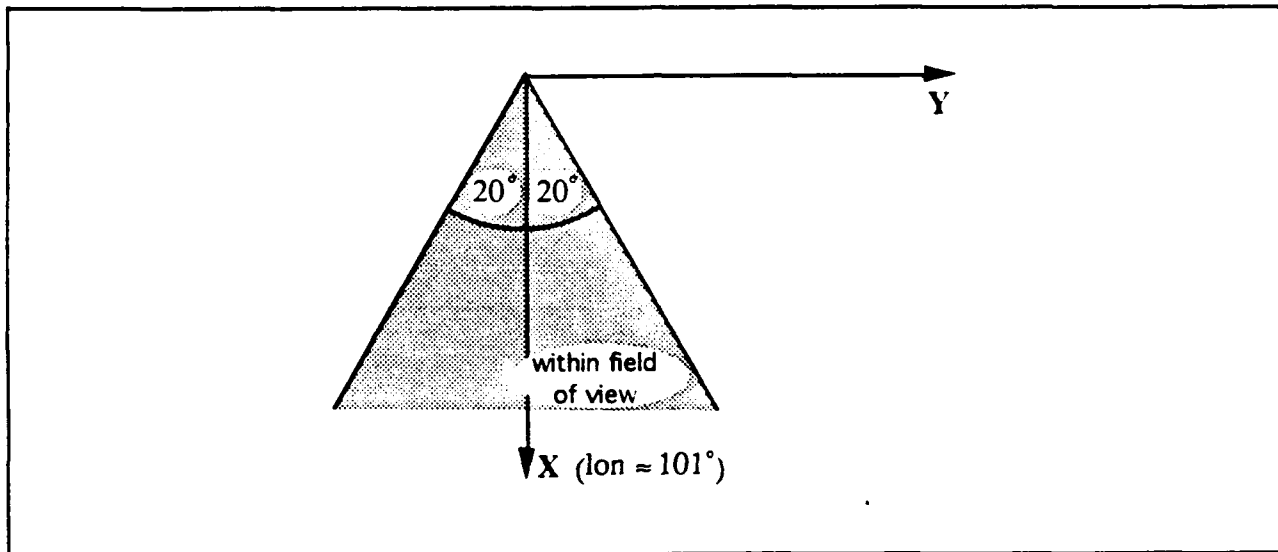


Figure 5.2. Sensor field of view.

#### D. ASSIMILATION OF OBSERVATIONS

Once a satellite is in the field of view of radar plane coverage, the input data file is checked for observations at or near its time of arrival. If a pair of direction

cosines is available, then a measurement estimate is calculated according to the development in App. B, where

$$\hat{z} = \begin{bmatrix} \rho_E / \rho \\ \rho_N / \rho \end{bmatrix} \quad (5.16)$$

$\hat{\Phi}$  is also calculated according to App. B. The plant noise covariance matrix  $Q$  is calculated using the squares of expected levels of uncertainty in each of the states. For example, if the two-body problem is the dynamic model, then the  $Q$  matrix would be

$$Q = \begin{bmatrix} \sigma_i^2 & 0 & 0 & 0 & 0 & 0 \\ 0 & \sigma_e^2 & 0 & 0 & 0 & 0 \\ 0 & 0 & \sigma_i^2 & 0 & 0 & 0 \\ 0 & 0 & 0 & \sigma_\Omega^2 & 0 & 0 \\ 0 & 0 & 0 & 0 & \sigma_\omega^2 & 0 \\ 0 & 0 & 0 & 0 & 0 & \sigma_M^2 \end{bmatrix} \quad (5.17)$$

where  $\sigma_n$  are proportional to the magnitude of the largest unmodeled perturbation, in the two-body case, earth oblateness. So, for the two-body problem,

$$\begin{bmatrix} \sigma_a \\ \sigma_e \\ \sigma_i \\ \sigma_\Omega \\ \sigma_\omega \\ \sigma_M \end{bmatrix} = \begin{bmatrix} \frac{3J_2 a}{2p^2} (1-e^2) \sin^2 i \cdot \cos[2(\omega + v)] \\ \frac{3J_2}{2p^2} \left(1 - \frac{3}{2} \sin^2 i\right) \cos v + \frac{1}{4} \sin^2 i \cdot \cos[2\omega + v] \\ \frac{3J_2}{8p^2} \sin 2i \cdot \cos[2(\omega + v)] \\ \frac{3J_2}{2p^2} n \cos i \cdot T_k \\ \frac{3J_2}{2p^2} n \left(2 - \frac{5}{2} \sin^2 i\right) T_k \\ \frac{3J_2}{2p^2} n \left(1 - \frac{3}{2} \sin^2 i\right) (1-e^2)^{1/2} T_k \end{bmatrix} \quad (5.18)$$

Now, the error covariance matrix can be calculated as

$$\mathbf{P}_{k/k-1} = \hat{\Phi} \mathbf{P}_{k-1/k-1} \hat{\Phi}^T + \mathbf{Q} \quad (5.19)$$

$\hat{\mathbf{H}}$  is then calculated as given in App. B, making possible the calculation of filter gain

$$\mathbf{G}_k = \mathbf{P}_{k/k-1} \hat{\mathbf{H}}^T (\hat{\mathbf{H}} \mathbf{P}_{k/k-1} \hat{\mathbf{H}}^T + \mathbf{R})^{-1} \quad (5.20)$$

which is then applied to the residuals  $\mathbf{z} - \hat{\mathbf{z}}$  to calculate improved orbital parameters  $\hat{\mathbf{x}}_{k/k}$ .

It should be noted that, throughout the filter, the quantities  $v$  and  $E$  are needed for various calculations.  $E$  is calculated from  $M$  using Newton-Rapson iteration on

$$M = E - e \sin E \quad (5.21)$$

and  $v$  is calculated by solving for

$$v = \sin^{-1} \left[ \frac{\sqrt{1-e^2} \sin E}{1-e \cos E} \right], \quad (5.22)$$

then using

$$v = \cos^{-1} \left[ \frac{\cos E - e}{1-e \cos E} \right] \quad (5.23)$$

to resolve the ambiguity.

## VI. RESULTS

This extended Kalman filter is designed to estimate the orbital parameters of a satellite, given observables in the form of a pair of direction cosines obtained upon the satellite's passage of an earth-fixed, stationary planar radar beam. One day's worth of data for each of three satellites was obtained for filter testing and adjustment. Results of the application of three successively more comprehensive filter models are compared with each other.

The first filter models only two-body motion, the second adds secular perturbations due to earth oblateness, and the third also includes periodic perturbations due to oblateness as well as atmospheric drag effects. Each filter, of course, models unknown perturbations as zero mean, white, Gaussian noise, in the tradition of Kalman filtering. Unfortunately, none of the available satellite data include an orbit in the drag regime. The filters will be compared in the areas of radar plane time of arrival, a residual small sample statistic, and orbital parameter estimation.

### A. RADAR PLANE TIME OF ARRIVAL

With orbiting objects arriving at the radar plane on the order of every few seconds, it is important that prediction of arrival times be fairly accurate. Current methods yield accuracies of within a second. The best that can be hoped for under the current detection configuration is about 0.25 second, which is the sensor time

uncertainty. After some crude tuning of the three filters, a comparison of arrival times for the three satellites is shown in Table 6.1, where  $\Delta t = t_{\text{obs}} - t_{\text{est}}$ .

It can be seen that, in all cases and for all models, the first detection time after the estimator is started up (which occurs on the order of 12 hours after filter initiation) is always mispredicted by the filter by a time on the order of seconds. However, it is seen that the secular and periodic models cut down that time error by a factor of from three to four. Subsequent detections yield differences in time between calculated and observed plane intersections of less than 1 second for a one-orbit-later detection and between two and three seconds if detection occurs next on the "backside" of the orbit (about a half day later). Although this is true

**Table 6.1. OBSERVED VS. ESTIMATED TIMES OF ARRIVAL.**

$\Delta t$ (sec)	2-body	Secular	Periodic
<b>Satellite 116</b>	13.94	4.29	4.30
	2.21	0.23	0.58
	-3.64	-2.61	-0.63
	-0.32	0.32	0.87
<b>Satellite 117</b>	15.18	4.76	4.78
	0.78	-0.10	0.17
	-0.13	-0.18	0.27
	-0.69	-2.40	-0.93
<b>Satellite 118</b>	12.39	3.49	3.49
	0.63	-0.01	0.21
	-2.24	-2.03	-0.81
	0.32	0.25	0.59

for the two-body and secular cases, the incorporation of periodic perturbations yields subsequent time differences of less than one second in all cases.

## B. RESIDUAL SMALL SAMPLE STATISTIC

The filter residual is the difference between actual and estimated observations, and, as such, is the basis for a good performance measure. The small sample variance of the residual is calculated for each case as follows:

$$\sigma^2 = \sum_{i=1}^n \frac{x_i^2}{n} - \bar{X}^2 \quad (6.1)$$

where

$$\bar{X} = \sum_{i=1}^n \frac{x_i}{n} \quad (6.2)$$

is the small sample mean,  $x_i$  being the  $i^{\text{th}}$  residual. Plots of these variances for each case are shown in figs. 6.1 - 6.3.

It is evident that the residuals for the N-S direction cosines are always very small. This is because this direction cosine is always close to  $90^\circ$  and the geometry of the problem always forces the estimate of this direction cosine to be very close to  $90^\circ$ . However, the E-W (in-plane) cosines are more interesting to observe. In general, the trend is toward smaller residual variances from observation to observation and from simple to more complex dynamic model. The only case where this does not hold true is for Satellite #117, where it can be seen that the two-body model is sufficiently lost after approximately eight hours to yield higher residuals than at the previous set of observations. Note that a "stack"

of asterisks denotes several observations gathered at the same radar plane crossing, which are then applied one at a time for parameter improvement.

It can be concluded from this limited residual data that, for the relatively short times included in the data, the filter is performing acceptably.

### **C. ORBITAL PARAMETER ESTIMATION**

The ultimate objective of this filter is to be able to predict what a satellite's position will be at some future time. Hopefully, the filter is predicting plane intersection times by accurately estimating orbital parameters. Figs. 6.4 - 6.6 show time propagating values of the four parameters that are expected to be varying most with respect to their two-body propagation values. All three satellites show similar results. In all cases, semi-major axis estimates differ greatly from model to model. Eccentricity estimates for the two-body and secular models are very similar, with the periodic model showing the greatest deviation. All estimates are very similar for the longitude of the ascending node, though, between observations, the two-body model does not have a mechanism to accurately propagate this element. Argument of perigee estimates are very close between the secular and periodic models, while the two-body makes very little correction to this parameter.

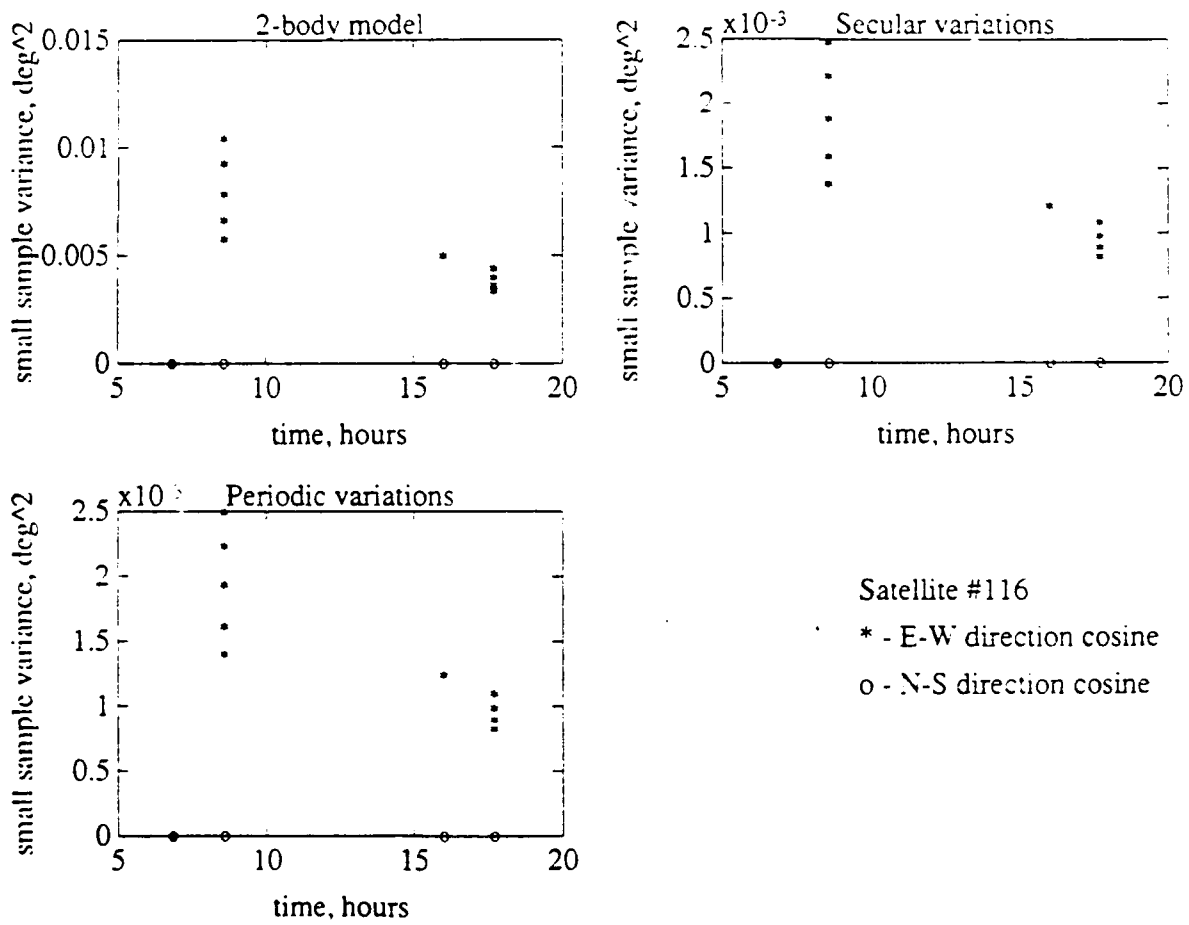


**Figure 6.1. Variance of residuals (sat. # 116).**

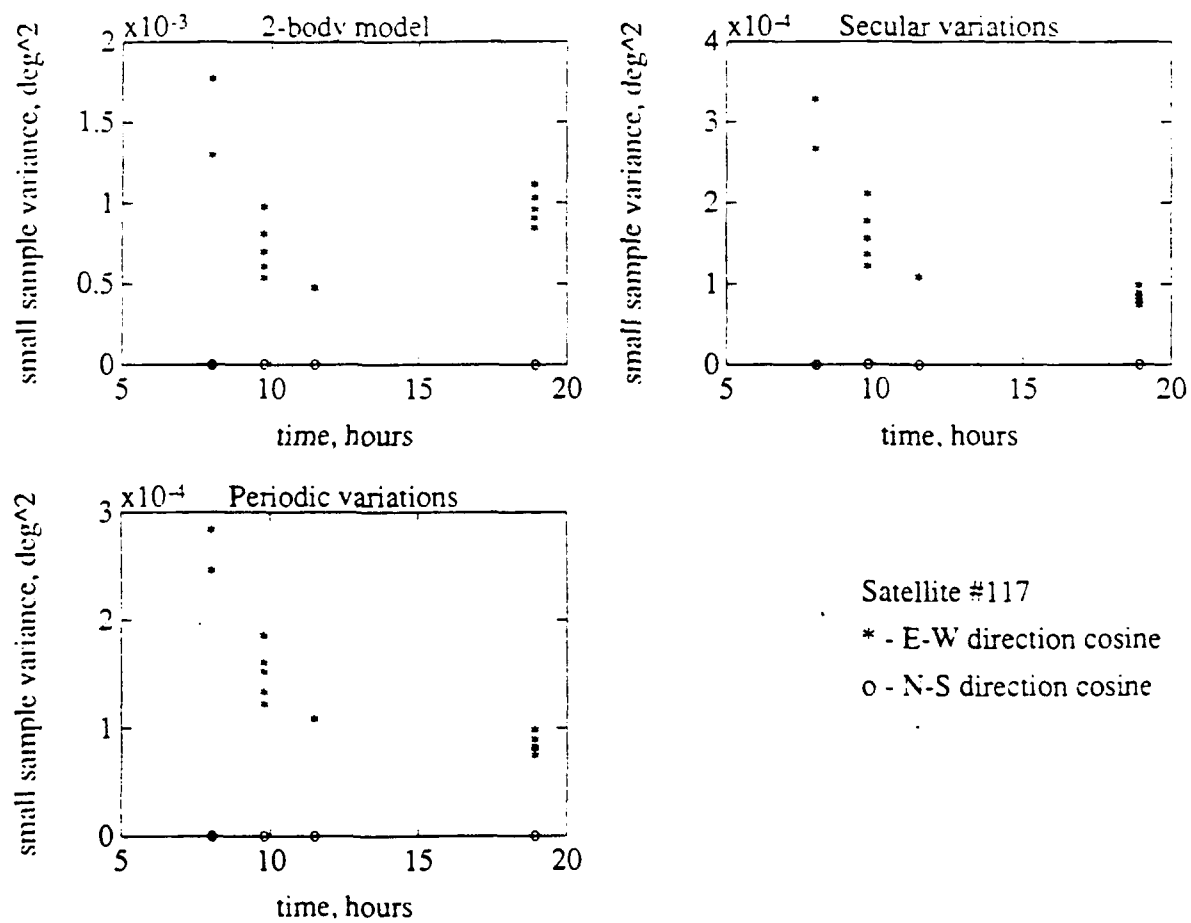


**Figure 6.2. Variance of residuals (sat. # 117).**

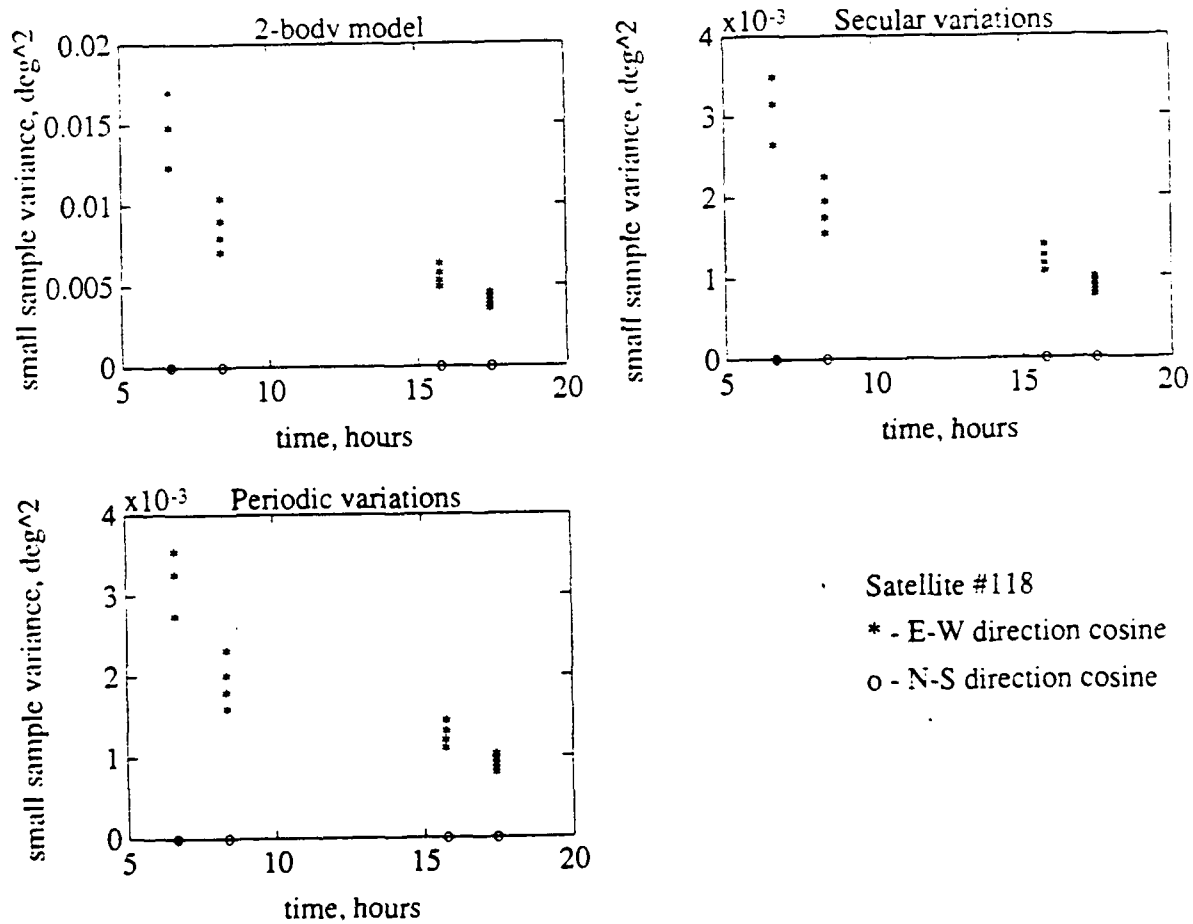


**Figure 6.3. Variance of residuals (sat. # 118).**

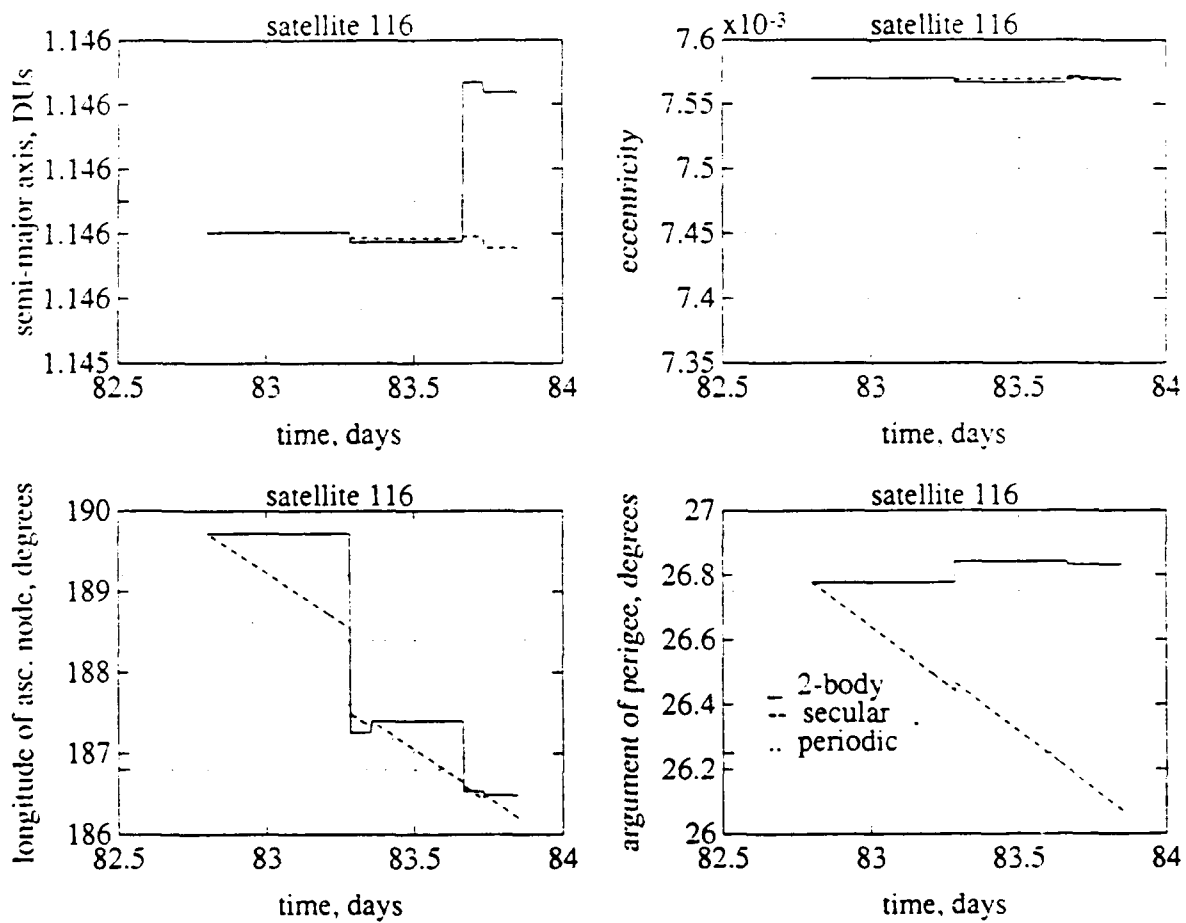


**Figure 6.4. Orbital element estimates (sat. # 116).**

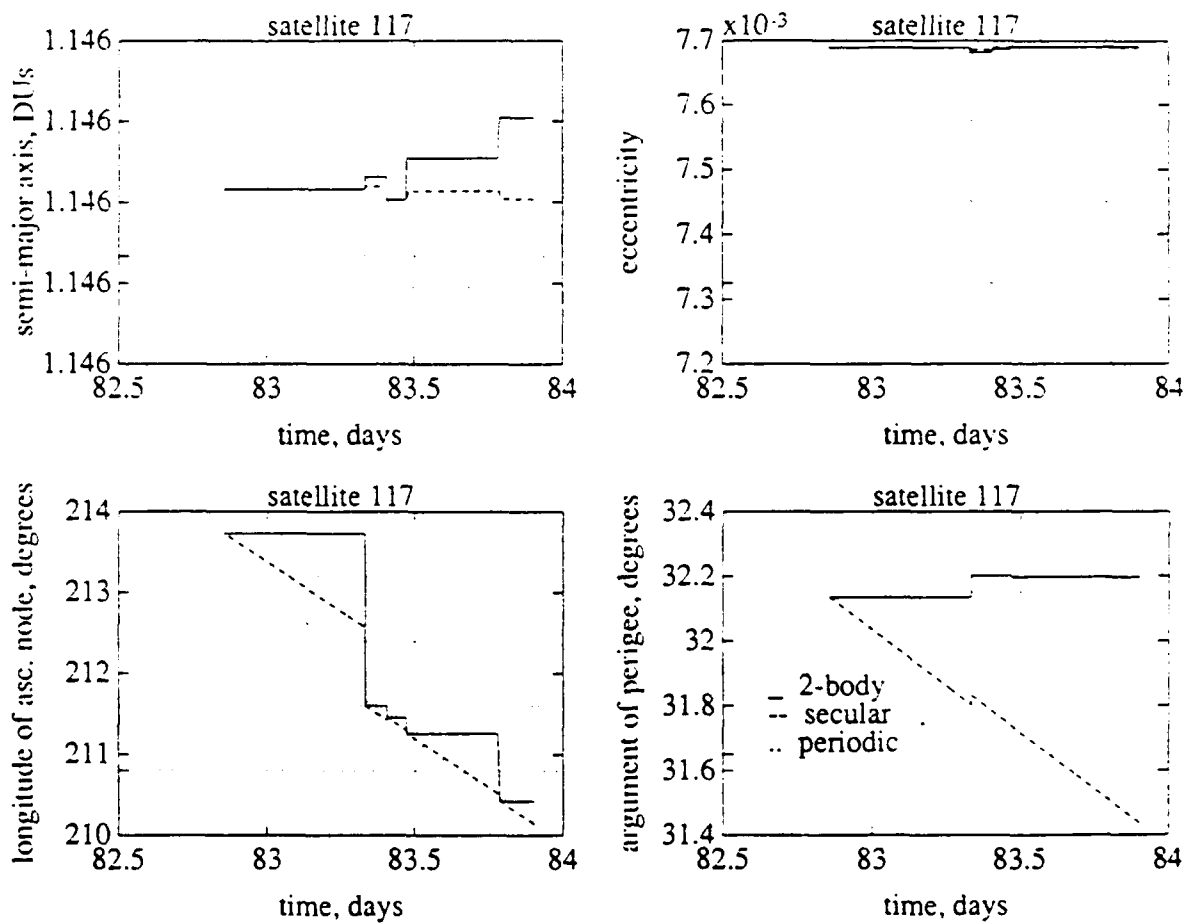


**Figure 6.5. Orbital element estimates (sat. # 117).**

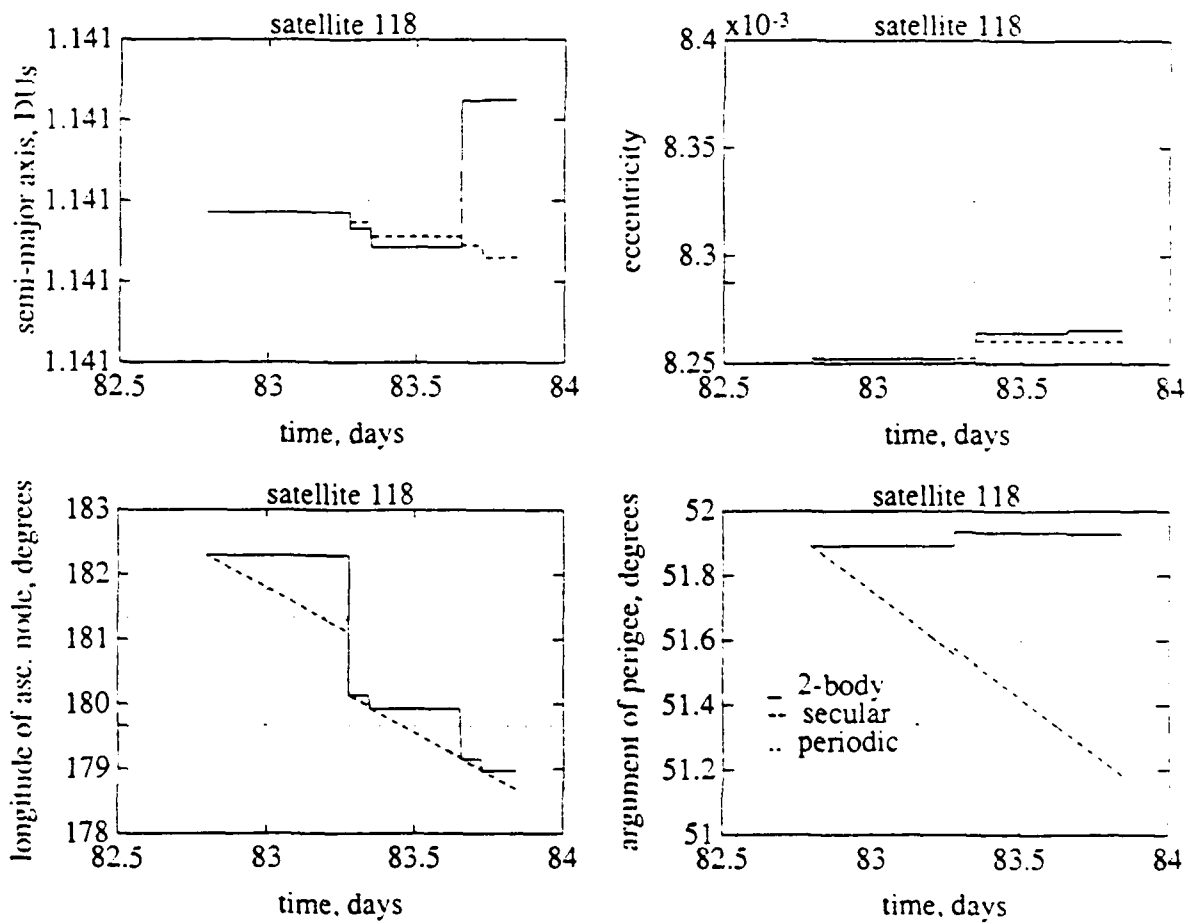


**Figure 6.6. Orbital element estimates (sat. # 118).**

## VII. CONCLUSIONS AND RECOMMENDATIONS

Orbital parameter estimation was attempted using an extended Kalman filter for each of three orbital dynamic models. Observations were angles only and made roughly twice a day per satellite passing through the radar plane. It was found that the two-body orbital model, including secular and periodic variations due to earth oblateness, was able to predict subsequent radar plane crossings to within a second of actual crossings.

The filter, which includes a crude model for atmospheric drag effects, was not tested on any satellites in the drag regime. Future research should include data from satellites with altitudes less than 600 km. Also, longer term data should be obtained to check filter performance over the long haul and also to see if the filter could track longer term disturbances or perturbations to the orbit under consideration.

Tuning of the filter could also be accomplished by obtaining a larger data base of satellite orbital elements and corresponding observations. This could be done manually, but it would be more exciting to see if an artificial neural network could be designed and trained to accomplish the same task.

## LIST OF REFERENCES

1. Bate, R. R., Mueller, D. D., and J. E. White, Fundamentals of Astrodynamics, Dover Publications, New York, 1971.
2. Danby, J. M. A., Fundamentals of Celestial Mechanics, Willmann-Bell Inc., Virginia, 1989.
3. Szebehely, V. G., Adventures in Celestial Mechanics, University of Texas Press, Texas, 1989.
4. Fitzpatrick, P. M., Principles of Celestial Mechanics, Academic Press, New York, 1970.
5. Geyling, F. T., and H. R. Westerman, Introduction to Orbital Mechanics, Addison-Wesley Publishing Company, Massachusetts, 1971.
6. Taff, L. G., Celestial Mechanics, John Wiley and sons, New York, 1985.
7. Solomon, D., "The NAVSPASUR Satellite Motion Model," Informational Document prepared for NRL under contract by Interferometrics Inc., August, 1991.
8. Brouwer, D., "Solution of the Problem of Artificial Satellite Theory Without Drag," The Astronomical Journal, Vol. 64, No. 1274, Nov. 1959, pp. 378-397.
9. Lyddane, R. H., "Small Eccentricities or Inclinations in the Brouwer Theory of the Artificial Satellite," The Astronomical Journal, Vol. 68, No. 8, Oct. 1963, pp. 555-558.
10. Cain, B. J., "Determination of Mean Elements for Brouwer's Satellite Theory," The Astronomical Journal, Vol. 67, No. 6, Aug. 1962, pp. 391-392.
11. Sochilina, A. S., "Some Modifications in Method of Improving the Orbits of Artificial Earth Satellites," AIAA Journal, Vol. 1, No. 12, Dec. 1963, pp. 2909-2911.
12. Easton, R. L., and J. J. Fleming, "The Navy Space Surveillance System," Proceedings of the IRE, April 1960, pp. 663-669.

13. Vahlberg, C. J., and A. C. Ramsay, "Improvements Related to Near-Earth Orbit Prediction," Final Report for NAVSPASUR by ST Systems Corp., Oct. 1990.
14. Schumacher, P. W., "Options for Improving Drag Calculations at NAVSPASUR," In-house paper, Analysis and Software Department, Dahlgren, VA, Mar 1988.
15. Brouwer, D., "Theoretical Evaluation of Atmospheric Drag Effects in the Motion of an Artificial Satellite," The Astronomical Journal, Vol. 66, No. 5, June 1961, pp. 193-225.
16. Zeleny, W. B., "Orbital Mechanics," Lecture Notes, Naval Postgraduate School, Jan. 1990.
17. Sorenson, H. W., Parameter Estimation, Marcel Dekker, Inc., New York, 1980.
18. Gelb, A., Applied Optimal Estimation, The M. I. T. Press, Massachusetts, 1974.
19. Kirk, D. E., Optimal Estimation: An Introduction to the Theory and Applications, Naval Postgraduate School, California, 1975.
20. Junkins, J. L., Orbit Estimation and Space Navigation, AIAA Professional Lecture Series, Mathematics and Methods of Astrodynamics, Minneapolis, Aug. 1988.
21. Hughes STX Corporation report prepared for NAVSPASUR, "Atmospherics Effects Task Final Kalman Filtering Results," Lanham, MD, July 1992.
22. Gibbs, B. ., "A Precision Recursive Estimate For Ephemeris Refinement (PREFER)," Proceedings of the Flight Mechanics/Estimation Theory Symposium, NASA Conference Publication 2123, Oct. 17-18, 1979.
23. Gunckel, T. L., "Orbit Determination Using Kalman's Method," Navigation Journal of the Institute of Navigation, Vol. 10, No. 3, Autumn 1963, pp. 273-291.

## APPENDIX A

### COORDINATE TRANSFORMATIONS

The calculations and algorithms presented in this paper necessitate describing vectors in several different coordinate frames. These frames are all orthogonal. Transformation of a vector from one reference frame's coordinates to another's is accomplished using direction cosine matrices (DCMs).

#### Reference Frames

The reference frames of interest are as follows (see fig. A.1):

***Geocentric inertial (IJK)*** - The **I** vector points inertially in the vernal equinox direction, with **I** and **J** lying in the equatorial plane, and **K** piercing the north pole (coincident with earth's spin axis).

***Orbit-fixed (PQW)*** - The orbital plane is the fundamental plane, with **P** pointing to perigee (point of closest approach), **Q** is the semi-latus rectum direction, and **W** is the orbit-normal (also orbital angular momentum direction).

***Radar plane (XYZ)*** - The radar plane is the fundamental plane, with **X** pointing to the maximum north latitude point, **Y** lies in the equatorial plane, and **Z** is the radar plane normal.

***Site-based (HEN)*** - **H** is local vertical, **E** is east, and **N** is north. The origin coincides with the radar site location of interest.

#### Direction Cosine Matrices

Three DCMs are developed here, performing one orthogonal rotation at a time, then combining the rotations.

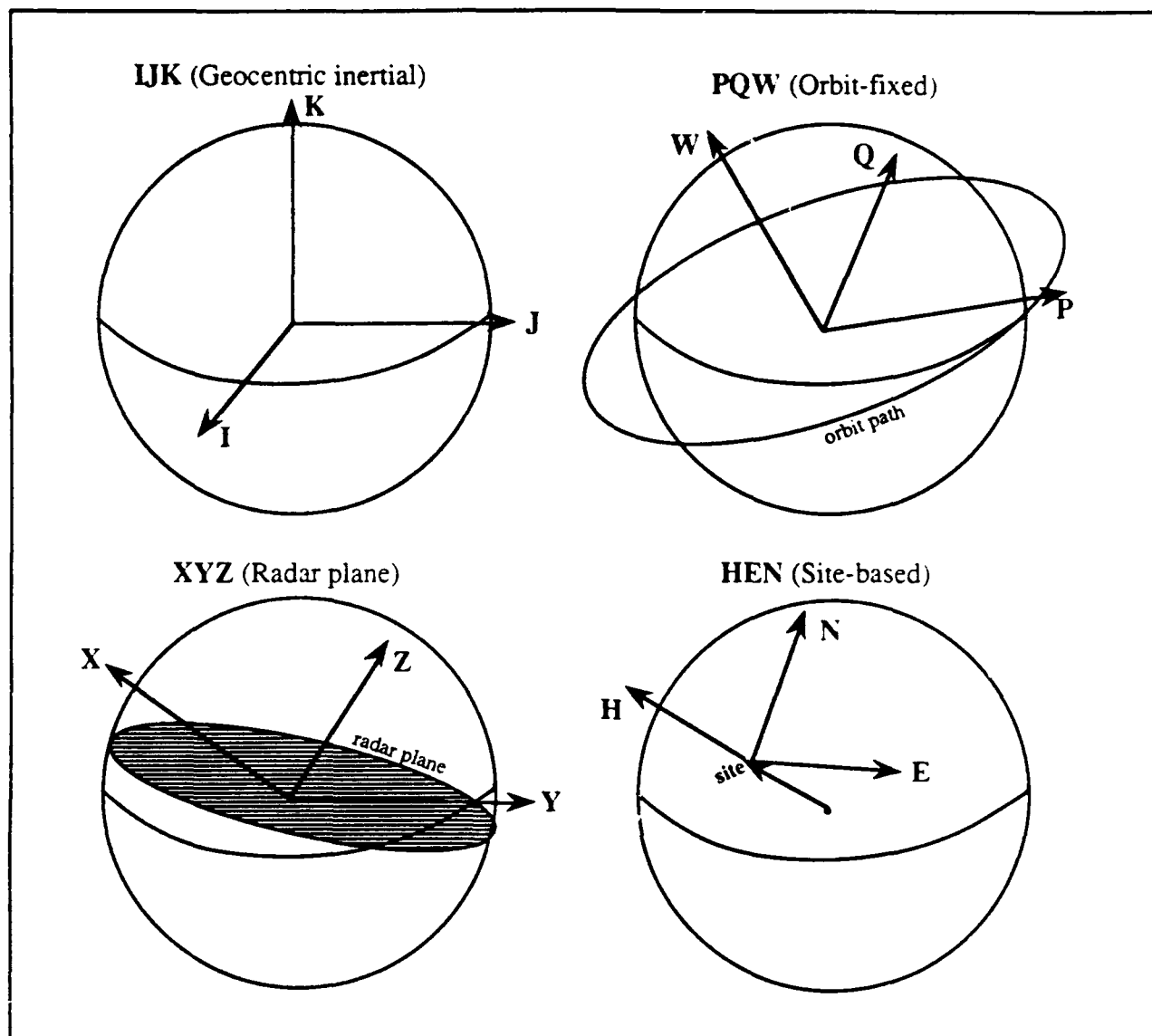
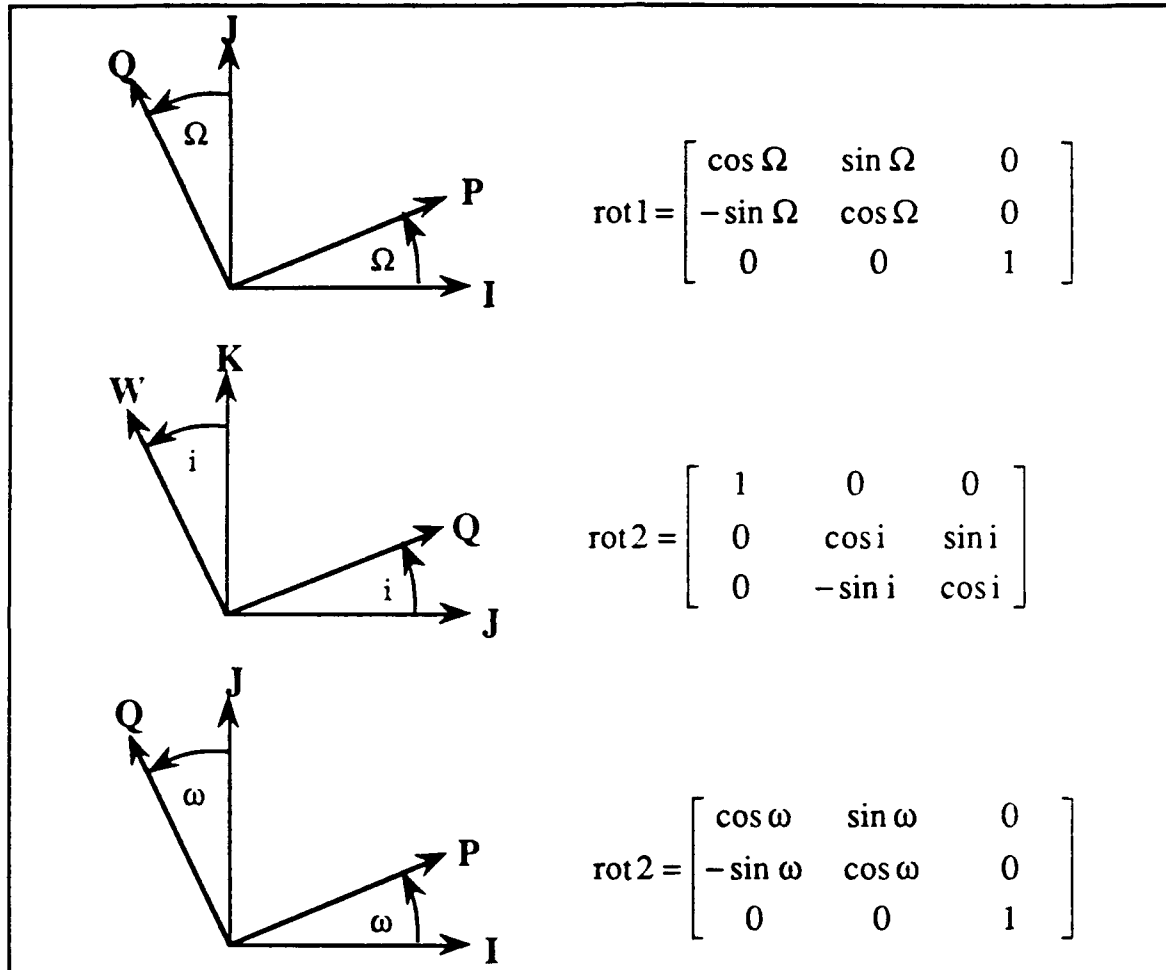


Figure A.1. Reference frames.

### *Orbit-fixed to Inertial*

Satellite position is most simply expressed in orbit-fixed coordinates, but for comparison with earth-fixed quantities, it is useful to transform both to an

intermediate reference frame. The inertial coordinate frame (in this case, geocentric inertial) is the obvious choice. Fig. A.2 shows the individual rotations required to transform a vector from orbit-fixed to inertial coordinates.



**Figure A.2. Orbit-fixed to inertial rotations.**

Combining the rotations yields

$$\begin{aligned} C^{\mathcal{P}/\mathcal{I}} &= [\text{rot3}][\text{rot2}][\text{rot1}] \\ &= \begin{bmatrix} c\omega c\Omega - s\omega s\Omega ci & c\omega s\Omega + s\omega c\Omega ci & s\omega si \\ -s\omega c\Omega - c\omega s\Omega ci & -s\omega s\Omega + c\omega c\Omega ci & c\omega si \\ s\Omega si & -si c\Omega & ci \end{bmatrix} \end{aligned} \quad (\text{A.1})$$

Because the transformation is orthogonal,

$$\begin{aligned} C^{\mathcal{I}/\mathcal{P}} &= [C^{\mathcal{P}/\mathcal{I}}]^T = \begin{bmatrix} c\omega c\Omega - s\omega s\Omega ci & -s\omega c\Omega - c\omega s\Omega ci & s\Omega si \\ c\omega s\Omega + s\omega c\Omega ci & -s\omega s\Omega + c\omega c\Omega ci & -si c\Omega \\ s\omega si & c\omega si & ci \end{bmatrix} \\ &= \begin{bmatrix} P_1 & P_2 & P_3 \\ P_4 & P_5 & P_6 \\ P_7 & P_8 & P_9 \end{bmatrix} \end{aligned} \quad (\text{A.2})$$

### *Inertial to Site-based*

Fig. A.3 shows the individual rotations required to transform a vector's coordinates from the inertial to a site-based reference frame. Rotation #1 keeps track of earth rotation. Rotation #3 points out the fact that the **E** and **N** vectors are not truly east- and north-pointing. **E** is in fact tangent to the great circle circumscribed by the radar plane, and **N** is orthogonal to **E** in the local horizontal plane.

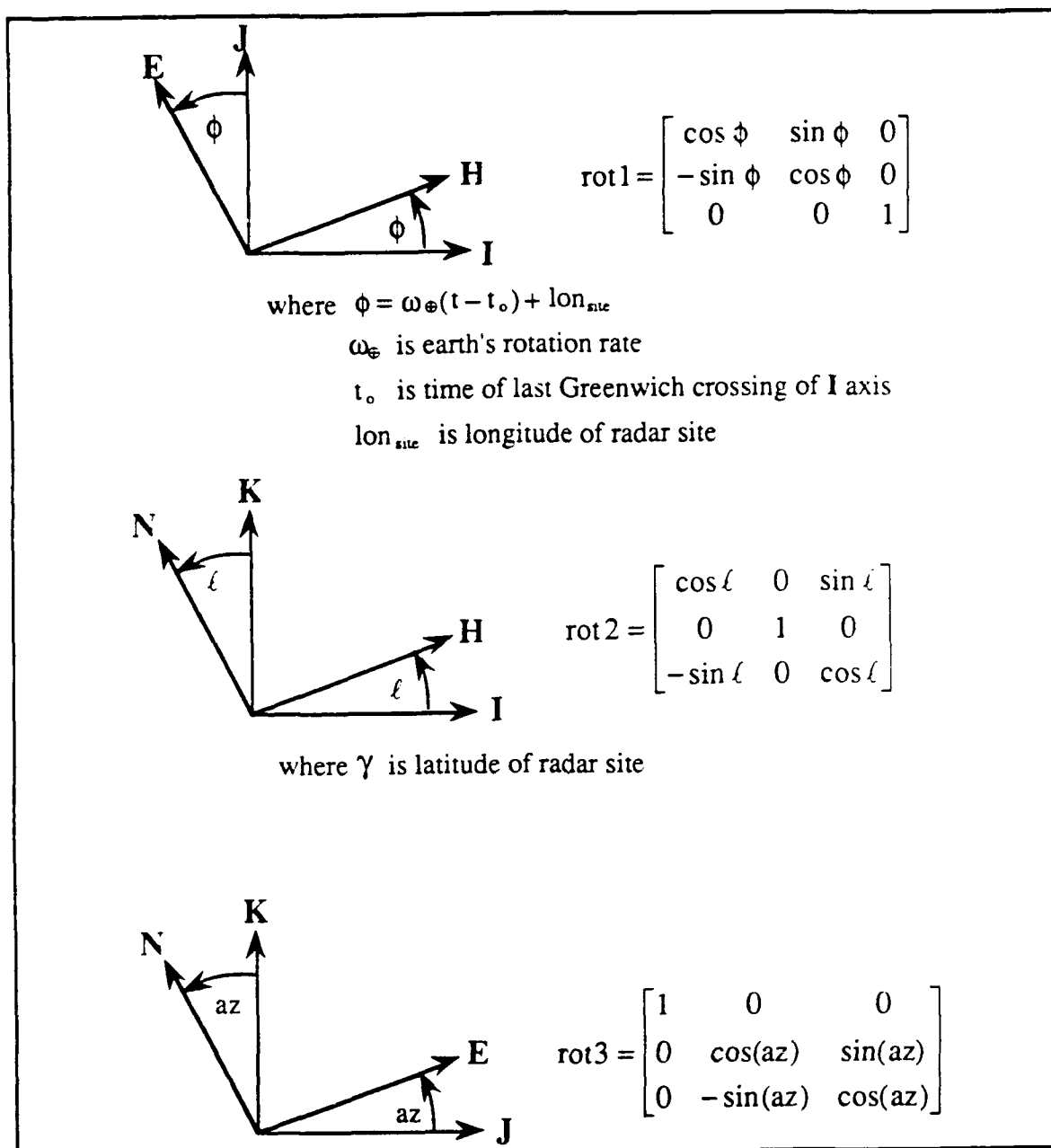


Figure A.3. Inertial to site-based rotations.

Combining the rotations yields

$$\begin{aligned} \mathbf{C}^{\mathcal{H}} &= [\text{rot3}][\text{rot2}][\text{rot1}] \\ &= \begin{bmatrix} c\ell c\phi & c\ell s\phi & s\ell \\ -s\phi c(\text{az}) - s\ell c\phi s(\text{az}) & c\phi c(\text{az}) - s(\text{az})s\ell s\phi & s(\text{az})c\ell \\ s\phi s(\text{az}) - s\ell c\phi c(\text{az}) & -c\phi s(\text{az}) - s\ell s\phi c(\text{az}) & c(\text{az})c\ell \end{bmatrix} \end{aligned} \quad (\text{A.3})$$

### ***Inertial to Radar Plane***

The transformation from inertial to radar plane coordinates is very useful to the determination of satellite crossings of the radar plane. Rotation #1 accounts for earth rotation. Fig. A.4 shows the individual rotations necessary to perform this transformation.

Combining these rotations yields

$$\mathbf{C}^{\mathcal{H}} = \begin{bmatrix} c\theta_{\pi} c\theta & c\theta_{\pi} s\theta & s\theta_{\pi} \\ -s\theta & c\theta & 0 \\ -s\theta_{\pi} c\theta & -s\theta_{\pi} s\theta & c\theta_{\pi} \end{bmatrix} \quad (\text{A.4})$$

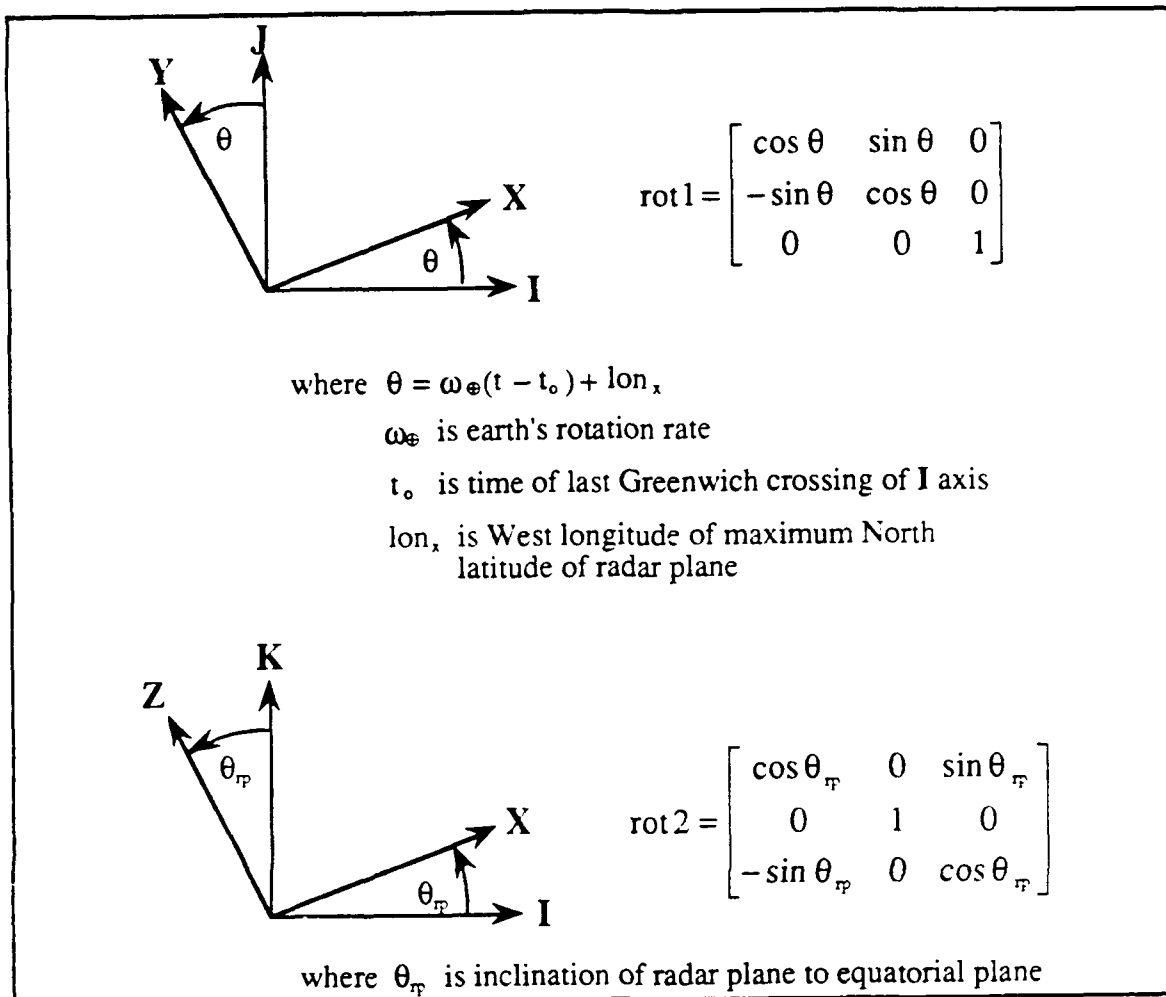


**Figure A.4. Inertial to radar plane rotations.**

## APPENDIX B

### LINEARIZED FILTER MATRICES $\hat{\Phi}$ AND $\hat{H}$

The extended Kalman filter can be viewed as a predictor-corrector type estimator. States are predicted using non-linear plant dynamics. Then a correction is computed by applying the Kalman gain to the filter residuals (observations minus estimates). Calculation of the Kalman gain requires some type of linearization of the plant and measurement dynamics (see eq. 3.18). Normally a Taylor series expansion is used, keeping only first order terms which are evaluated at the best current state estimate. The general form of the linearization of a nonlinear discrete function

$$\mathbf{x}_{k+1} = f(\mathbf{x}_k, T_k) = \begin{bmatrix} f_1(\mathbf{x}_k, T_k) \\ f_2(\mathbf{x}_k, T_k) \\ \vdots \\ f_m(\mathbf{x}_k, T_k) \end{bmatrix} \quad (\text{B.1})$$

is

$$\hat{\Phi} = \begin{bmatrix} \frac{\partial f_1}{\partial x_{1k}} & \frac{\partial f_1}{\partial x_{2k}} & \dots & \frac{\partial f_1}{\partial x_{n_k}} \\ \frac{\partial f_2}{\partial x_{1k}} & \ddots & & \vdots \\ \vdots & & \ddots & \vdots \\ \frac{\partial f_m}{\partial x_{1k}} & \dots & \dots & \frac{\partial f_m}{\partial x_{n_k}} \end{bmatrix}_{\mathbf{x}_k = \hat{\mathbf{x}}_{k-1}} \quad (\text{B.2})$$

## Development of Linear Plant Matrix $\hat{\Phi}$

As will be seen, the state matrix  $\hat{\Phi}$  can be as complex as one lets it become. Following is a presentation of three progressively more complex models;

- 1) Keplerian two-body motion,
- 2) inclusion of dominant first order earth oblateness gravity effects, and
- 3) dominant atmospheric drag effects.

### *Two-Body Problem*

State dynamics for a Keplerian 2-body orbit are given as

$$\begin{bmatrix} a_{k+1} \\ e_{k+1} \\ i_{k+1} \\ \Omega_{k+1} \\ \omega_{k+1} \\ M_{k+1} \end{bmatrix} = \begin{bmatrix} a_k \\ e_k \\ i_k \\ \Omega_k \\ \omega_k \\ M_k + a_k^{-3/2} T_k \end{bmatrix} = f(\mathbf{x}_k, T_k) \quad (\text{B.3})$$

Linearizing gives

$$\hat{\Phi} = \begin{bmatrix} 1 & 0 & 0 & 0 & 0 & 0 \\ 0 & 1 & 0 & 0 & 0 & 0 \\ 0 & 0 & 1 & 0 & 0 & 0 \\ 0 & 0 & 0 & 1 & 0 & 0 \\ 0 & 0 & 0 & 0 & 1 & 0 \\ -\frac{3}{2} a_k^{-5/2} T_k & 0 & 0 & 0 & 0 & 1 \end{bmatrix} \quad (\text{B.4})$$

### *Secular Variations Due to Earth's Oblateness*

To first order, the last three orbital elements are affected by secular variations, so that

$$\mathbf{x}_{k+1} = \begin{bmatrix} a_k \\ e_k \\ i_k \\ \Omega_k - \frac{3J_2}{2p_k^2} (\cos i_k) \Delta v \\ \omega_k + \frac{3J_2}{2p_k^2} \left( 2 - \frac{5}{2} \sin^2 i_k \right) \Delta v \\ M_k + a_k^{-3/2} \left[ 1 + \frac{J_2 a_k}{r_k^3} (1 - 3 \sin^2 \delta_k) \right]^{3/2} T_k \end{bmatrix} = f(\mathbf{x}_k, T_k) \quad (\text{B.5})$$

where

$$r_k = \frac{p_k}{1 + e_k \cos v_k} \quad (\text{B.6})$$

$$\sin \delta_k = \sin i_k \sin(v_k + \omega_k)$$

Linearizing gives

$$\hat{\Phi} = \begin{bmatrix} 1 & 0 & 0 & 0 & 0 & 0 \\ 0 & 1 & 0 & 0 & 0 & 0 \\ 0 & 0 & 1 & 0 & 0 & 0 \\ \frac{\partial \Omega_{k+1}}{\partial a_k} & \frac{\partial \Omega_{k+1}}{\partial e_k} & \frac{\partial \Omega_{k+1}}{\partial i_k} & 1 & 0 & \frac{\partial \Omega_{k+1}}{\partial M_k} \\ \frac{\partial \omega_{k+1}}{\partial a_k} & \frac{\partial \omega_{k+1}}{\partial e_k} & \frac{\partial \omega_{k+1}}{\partial i_k} & 0 & 1 & \frac{\partial \omega_{k+1}}{\partial M_k} \\ \frac{\partial M_{k+1}}{\partial a_k} & \frac{\partial M_{k+1}}{\partial e_k} & \frac{\partial M_{k+1}}{\partial i_k} & 0 & \frac{\partial M_{k+1}}{\partial \omega_k} & \frac{\partial M_{k+1}}{\partial M_k} \end{bmatrix}_{k, k+1} \quad (\text{B.7})$$

where the terms in the fourth row are found to be

$$\begin{aligned} \frac{\partial \Omega_{k+1}}{\partial a_k} &= \frac{3J_2}{p_k^3} \cos i_k \Delta v \frac{\partial p_k}{\partial a_k} \\ \frac{\partial \Omega_{k+1}}{\partial e_k} &= \frac{3J_2}{p_k^3} \cos i_k \Delta v \frac{\partial p_k}{\partial e_k} \\ \frac{\partial \Omega_{k+1}}{\partial i_k} &= \frac{3J_2}{2p_k^2} \sin i_k \Delta v \\ \frac{\partial \Omega_{k+1}}{\partial M_k} &= \frac{3J_2}{2p_k^2} \cos i_k \frac{\partial v_k}{\partial M_k} \end{aligned} \quad (\text{B.8})$$

where

$$\begin{aligned}\frac{\partial p_k}{\partial a_k} &= 1 - e_k^2 \\ \frac{\partial p_k}{\partial e_k} &= -2ae\end{aligned}\tag{B.9}$$

$$\frac{\partial v_k}{\partial M_k} = \frac{1(1 + e^2) \sin E + 2e \sin E \cos E}{-\sin v_k (1 - e \cos E)^3}$$

The fifth row terms are found to be

$$\begin{aligned}\frac{\partial \omega_{k+1}}{\partial a_k} &= \frac{-3J_2}{p_k^3} A_{3\bullet} \Delta v \frac{\partial p_k}{\partial a_k} \\ \frac{\partial \omega_{k+1}}{\partial e_k} &= \frac{-3J_2}{p_k^3} A_{3\bullet} \Delta v \frac{\partial p_k}{\partial e_k} \\ \frac{\partial \omega_{k+1}}{\partial i_k} &= \frac{-15J_2}{2p_k^2} \sin i_k \cos i_k \Delta v \\ \frac{\partial \omega_{k+1}}{\partial M_k} &= \frac{-3J_2}{2p_k^2} A_{3\bullet} \frac{\partial v_k}{\partial M_k}\end{aligned}\tag{B.10}$$

where

$$A_{3\bullet} = 2 - \frac{5}{2} \sin^2 i\tag{B.11}$$

Sixth row terms can be evaluated by

$$\begin{aligned}
\frac{\partial M_{k+1}}{\partial a_k} &= \frac{-9J_2}{2r_k^4} A_{4\bullet} A_{6\bullet} T_k \frac{\partial r_k}{\partial a_k} \\
\frac{\partial M_{k+1}}{\partial e_k} &= \frac{-9J_2}{2r_k^4} A_{4\bullet} A_{6\bullet} T_k \frac{\partial r_k}{\partial e_k} \\
\frac{\partial M_{k+1}}{\partial i_k} &= \frac{-9J_2}{r_k^3} A_{6\bullet} \sin \delta_k T_k \frac{\partial(\sin \delta_k)}{\partial i_k} \\
\frac{\partial M_{k+1}}{\partial \omega_k} &= \frac{-9J_2}{r_k^3} A_{6\bullet} \sin \delta_k T_k \frac{\partial(\sin \delta_k)}{\partial \omega_k} \\
\frac{\partial M_{k+1}}{\partial M_k} &= 1 + \frac{3}{2} A_{6\bullet} T_k \frac{\partial A_{8\bullet}}{\partial v_k} \frac{\partial v_k}{\partial M_k}
\end{aligned} \tag{B.12}$$

where

$$\begin{aligned}
\frac{\partial r_k}{\partial a_k} &= \frac{A_{5\bullet}}{A_{7\bullet}} \\
\frac{\partial r_k}{\partial e_k} &= \frac{-2a_k e_k A_{7\bullet} - p_k \cos v_k}{A_{7\bullet}^2} \\
\frac{\partial A_{8\bullet}}{\partial v_k} &= \frac{-3J_2}{r_k^4} \left[ \frac{\partial r_k}{\partial v_k} + 3 \sin^2 \delta_k \frac{\partial r_k}{\partial v_k} - 2r_k \sin \delta_k \frac{\partial(\sin \delta_k)}{\partial v_k} \right] \\
\frac{\partial r_k}{\partial v_k} &= \frac{a_k (1 - e_k^2) e_k \sin v_k}{(1 + e \cos v_k)^2} \\
\frac{d(\sin \delta_k)}{\partial v_k} &= \sin i_k \cos(v_k + \omega_k)
\end{aligned} \tag{B.13}$$

and

$$\begin{aligned}
 A_{4\bullet} &= 1 - 3 \sin^2 \delta_k \\
 A_{5\bullet} &= 1 - e_k^2 \\
 A_{6\bullet} &= \left( 1 + \frac{J_2}{r_k^3} A_{4\bullet} \right)^{1/2} \\
 A_{7\bullet} &= 1 + e_k \cos v_k \\
 A_{8\bullet} &= \frac{J_2}{r_k^3} (1 - 3 \sin^2 \delta_k)
 \end{aligned} \tag{B.14}$$

### Development of $\hat{z}$ and $\hat{H}$

The relationship between the measurements (pseudo-observables) and orbital parameters (filter states) is contained in the nonlinear function

$$z_k = g(x_k, T_k) \tag{B.15}$$

and is the same regardless of the state dynamics model being considered. The observables of interest here are the north-south and east-west direction cosines, or

$$z = \begin{bmatrix} \cos \alpha \\ \cos \beta \end{bmatrix} \tag{B.16}$$

and are related to the range vector  $\bar{\rho}$  by

$$\begin{bmatrix} \cos \alpha \\ \cos \beta \end{bmatrix} = \begin{bmatrix} \rho_E / \rho \\ \rho_N / \rho \end{bmatrix} \tag{B.17}$$

Note (from fig. B.1) that the **HEN** coordinate system in which  $\rho$  is received is not truly up, east and north. **H** is local vertical, but **E** is tangent to the radar plane great circle, and **N** is orthogonal to **E** in the local horizontal plane. This site-dependent information is included in the transformation matrix  $C^H$  (see App. A) as the angle  $\alpha$  between true east and **E**.

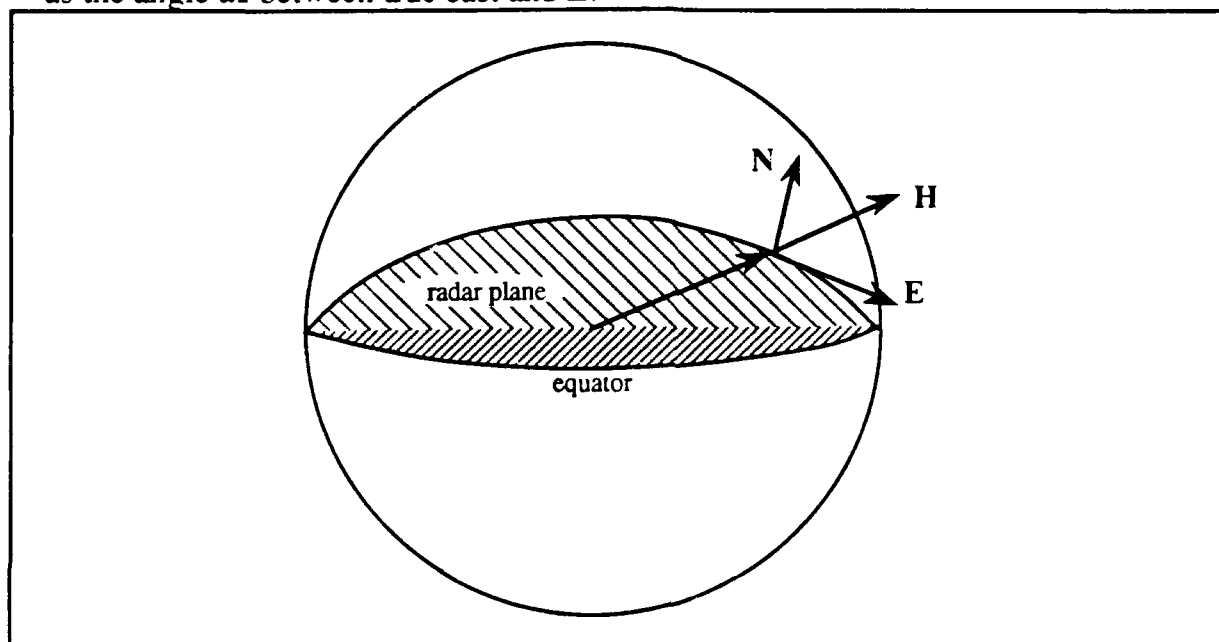


**Figure B.1. Site-based coordinate system.**

So  $\rho_E$ ,  $\rho_N$ , and range magnitude  $\rho$  need to be expressed in terms of the orbital parameters in order to form  $z = g(x, T)$ . It can be stated that

$$\bar{\rho} = \begin{bmatrix} \rho_H \\ \rho_E \\ \rho_N \end{bmatrix} = \begin{bmatrix} \rho \cos \gamma \\ \rho \cos \alpha \\ \rho \cos \beta \end{bmatrix} \quad (B.18)$$

In order to describe the direction cosines in terms of orbital parameters, first consider fig. B.2. Earth's flattening has been exaggerated in the figure to clearly show the effect on radar plane orientation. From the figure, it is clear that

$$\mathbf{r} = \mathbf{r}_{\text{offset}} + \mathbf{R}_{\text{site}} + \bar{\rho} \quad (\text{B.19})$$

where

$$\begin{aligned} R_{\text{site}} &= R(\text{lat}) + \text{alt}_{\text{site}} \\ R(\text{lat}) &= \sqrt{1 - \left[ \frac{2 - 1/298.26}{298.26} \right] \sin^2(\text{lat})} \\ r_{\text{offset}} &\approx 20\text{km} \end{aligned} \quad (\text{B.20})$$

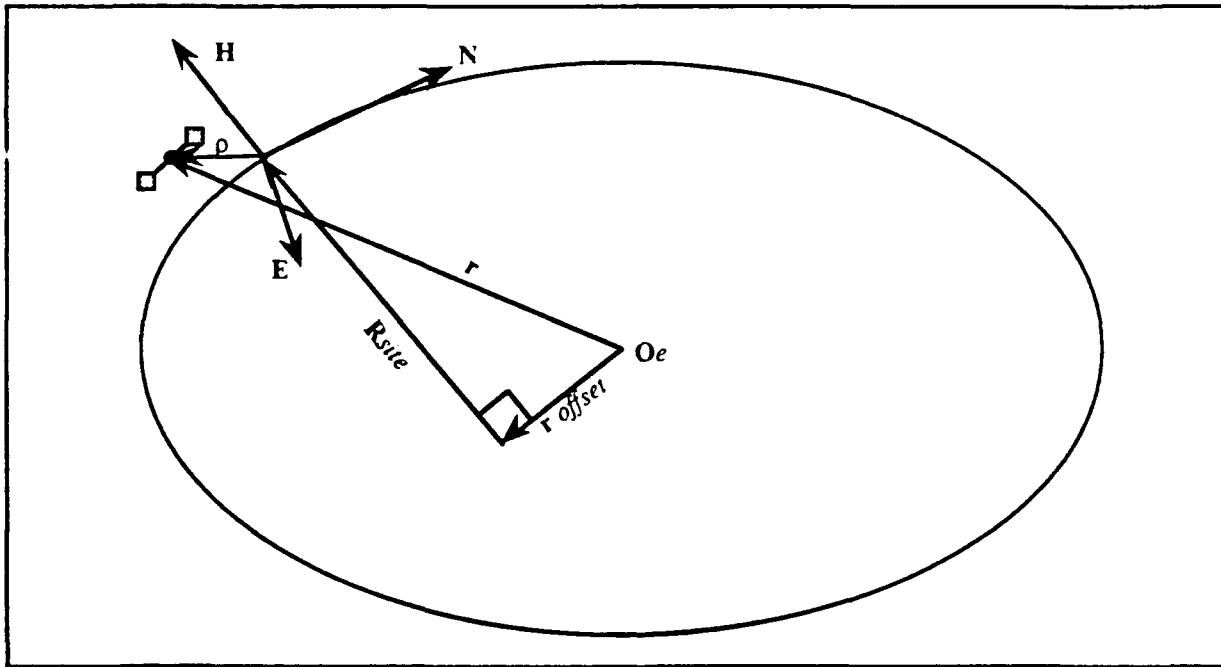


**Figure B.2. Relationship between satellite position and range.**

$R(\text{lat})$  is the latitude dependent radius of a point on the reference geoid (due to flattening) [7] and is assumed to be in the  $\mathbf{H}$  direction.  $r_{\text{offset}}$  is assumed to be totally in the negative  $\mathbf{N}$  direction, and  $\text{alt}_{\text{site}}$  is the receiver's altitude. Combining the elements of eqs. B.18 and B.19 yields

$$\mathbf{r}^H = \begin{bmatrix} R_{\text{site}} + \rho \cos \gamma \\ \rho \cos \alpha \\ -r_{\text{offset}} + \rho \cos \beta \end{bmatrix} \quad (\text{B.21})$$

$\mathbf{r}^H$  is the transformation of  $\mathbf{r}^P$  from the orbit-fixed coordinate system to site-based coordinates, or

$$\begin{aligned} \mathbf{r}^H &= \mathbf{C}^H \mathbf{C}^P \mathbf{r}^P \\ &= \begin{bmatrix} H_1 & H_2 & H_3 \\ H_4 & H_5 & H_6 \\ H_7 & H_8 & H_9 \end{bmatrix} \begin{bmatrix} P_1 & P_2 & P_3 \\ P_4 & P_5 & P_6 \\ P_7 & P_8 & P_9 \end{bmatrix} \begin{bmatrix} r \cos v \\ r \sin v \\ 0 \end{bmatrix} \\ &= \begin{bmatrix} r(R_7 \cos v + R_8 \sin v) \\ r(R_1 \cos v + R_2 \sin v) \\ r(R_4 \cos v + R_5 \sin v) \end{bmatrix} \end{aligned} \quad (\text{B.22})$$

where

$$\begin{aligned} R_1 &= H_4 P_1 + H_5 P_4 + H_6 P_7 \\ R_2 &= H_4 P_2 + H_5 P_5 + H_6 P_8 \\ R_4 &= H_7 P_1 + H_8 P_4 + H_9 P_7 \\ R_5 &= H_7 P_2 + H_8 P_5 + H_9 P_8 \\ R_7 &= H_1 P_1 + H_2 P_4 + H_3 P_7 \\ R_8 &= H_1 P_2 + H_2 P_5 + H_3 P_8 \end{aligned} \quad (\text{B.23})$$

Combining eqs. B.18, B.21, and B.22 yields

$$\begin{bmatrix} \rho_H \\ \rho_E \\ \rho_N \end{bmatrix} = \begin{bmatrix} r(R_7 \cos v + R_8 \sin v) - R_{\text{site}} \\ r(R_1 \cos v + R_2 \sin v) \\ r(R_4 \cos v + R_5 \sin v) + r_{\text{offset}} \end{bmatrix} \quad (\text{B.24})$$

From eq. B.24,  $\rho$  can be calculated as

$$\rho = \sqrt{\rho_H^2 + \rho_E^2 + \rho_N^2} \quad (\text{B.25})$$

Now, eq. B.15 can be used as the estimate of the observation to compute filter residuals. But the Kalman gain depends on the matrix  $\hat{\mathbf{H}}$ , which is derived by linearizing  $g(\mathbf{x}_k, T_k)$  with respect to  $\mathbf{x}_k$ .

The form of  $\hat{\mathbf{H}}$  is as follows

$$\hat{\mathbf{H}} = \begin{bmatrix} \frac{\partial(\rho_E/\rho)}{\partial a} & \dots & \dots & \frac{\partial(\rho_E/\rho)}{\partial M} \\ \frac{\partial(\rho_N/\rho)}{\partial a} & \dots & \dots & \frac{\partial(\rho_N/\rho)}{\partial M} \end{bmatrix} \quad (\text{B.26})$$

where

$$\begin{aligned}
\frac{\partial(\rho_E/\rho)}{\partial a} &= \frac{1}{\rho} \frac{\partial \rho_E}{\partial a} - \rho_E \frac{1}{\rho^2} \frac{\partial \rho}{\partial a} \\
&\vdots \\
\frac{\partial(\rho_E/\rho)}{\partial M} &= \frac{1}{\rho} \frac{\partial \rho_E}{\partial M} - \rho_E \frac{1}{\rho^2} \frac{\partial \rho}{\partial M} \\
\frac{\partial(\rho_N/\rho)}{\partial a} &= \frac{1}{\rho} \frac{\partial \rho_N}{\partial a} - \rho_N \frac{1}{\rho^2} \frac{\partial \rho}{\partial a} \\
&\vdots \\
\frac{\partial(\rho_N/\rho)}{\partial M} &= \frac{1}{\rho} \frac{\partial \rho_N}{\partial M} - \rho_N \frac{1}{\rho^2} \frac{\partial \rho}{\partial M}
\end{aligned} \tag{B.27}$$

Following are the details of this development.

$$\begin{aligned}
\frac{\partial \rho_E}{\partial a} &= (R_1 \cos v + R_2 \sin v) \frac{\partial r}{\partial a} \\
\frac{\partial \rho_H}{\partial a} &= (R_7 \cos v + R_8 \sin v) \frac{\partial r}{\partial a} \\
\frac{\partial \rho_N}{\partial a} &= (R_4 \cos v + R_5 \sin v) \frac{\partial r}{\partial a} \\
\frac{\partial \rho}{\partial a} &= \frac{1}{\rho} \left( \rho_H \frac{\partial \rho_H}{\partial a} + \rho_E \frac{\partial \rho_E}{\partial a} + \rho_N \frac{\partial \rho_N}{\partial a} \right)
\end{aligned} \tag{B.28}$$

where

$$\frac{\partial r}{\partial a} = \frac{1 - e^2}{1 + e \cos v} \quad (\text{B.29})$$

The expressions for the change in  $\rho$  with respect to eccentricity  $e$  are identical to eq. B.28 except for the replacement of  $\partial r / \partial a$  with  $\partial r / \partial e$ , which is

$$\frac{\partial r}{\partial e} = \frac{-a(2e + \cos v + e^2 \cos v)}{(1 + e \cos v)^2} \quad (\text{B.30})$$

Since the  $R_n$  terms in eq B.24 are functions of the orbital elements  $i$ ,  $\Omega$ , and  $\omega$ , the expressions for the change in  $\rho$  with respect to these three elements are as follows, with the replacement of  $\partial \zeta$  by the appropriate element:

$$\begin{aligned} \frac{\partial \rho_E}{\partial \zeta} &= \left( \frac{\partial R_7}{\partial \zeta} \cos v + \frac{\partial R_8}{\partial \zeta} \sin v \right) r \\ \frac{\partial \rho_E}{\partial \zeta} &= \left( \frac{\partial R_1}{\partial \zeta} \cos v + \frac{\partial R_2}{\partial \zeta} \sin v \right) r \\ \frac{\partial \rho_N}{\partial \zeta} &= \left( \frac{\partial R_4}{\partial \zeta} \cos v + \frac{\partial R_5}{\partial \zeta} \sin v \right) r \\ \frac{\partial \rho}{\partial a} &= \frac{1}{\rho} \left( \rho_H \frac{\partial \rho_H}{\partial \zeta} + \rho_E \frac{\partial \rho_E}{\partial \zeta} + \rho_N \frac{\partial \rho_N}{\partial \zeta} \right) \end{aligned} \quad (\text{B.31})$$

The expressions for the change in  $\rho$  with respect to a change in mean anomaly  $M$  is more involved because of the relationship between mean and true anomalies. This relationship is repeated here for convenience:

$$M = E - e \sin E \quad (B.32)$$

$$\cos v = \frac{\cos E - e}{1 - e \cos E} \quad (B.33)$$

$$\sin v = \frac{\sin E \sqrt{1 - e^2}}{1 - e \cos E} \quad (B.34)$$

Taking partial derivatives as appropriate yields

$$\begin{aligned} \frac{\partial \rho_H}{\partial M} &= \left[ R_7 \frac{\partial(\cos v)}{\partial M} + R_8 \frac{\partial(\sin v)}{\partial M} \right] r + [R_7 \cos v + R_8 \sin v] \frac{\partial r}{\partial M} \\ \frac{\partial \rho_E}{\partial M} &= \left[ R_1 \frac{\partial(\cos v)}{\partial M} + R_2 \frac{\partial(\sin v)}{\partial M} \right] r + [R_1 \cos v + R_2 \sin v] \frac{\partial r}{\partial M} \\ \frac{\partial \rho_N}{\partial M} &= \left[ R_4 \frac{\partial(\cos v)}{\partial M} + R_5 \frac{\partial(\sin v)}{\partial M} \right] r + [R_4 \cos v + R_5 \sin v] \frac{\partial r}{\partial M} \end{aligned} \quad (B.35)$$

$$\frac{\partial \rho}{\partial M} = \frac{1}{\rho} \left[ \rho_H \frac{\partial \rho_H}{\partial M} + \rho_E \frac{\partial \rho_E}{\partial M} + \rho_N \frac{\partial \rho_N}{\partial M} \right]$$

where

$$\frac{\partial(\cos v)}{\partial M} = -\sin v \frac{\partial v}{\partial E} \frac{\partial E}{\partial M}$$

$$\frac{\partial(\sin v)}{\partial M} = \cos v \frac{\partial v}{\partial E} \frac{\partial E}{\partial M}$$

$$\frac{\partial r}{\partial M} = \frac{ae(1-e^2)\sin v}{(1+e\cos v)^2} \frac{\partial v}{\partial E} \frac{\partial E}{\partial M}$$

$$\frac{\partial v}{\partial E} = \frac{-(1+e^2)\sin E + 2e\sin E\cos E}{-\sin v(1-e\cos E)^2}$$

(B.36)

$$\frac{\partial E}{\partial M} = \frac{1}{1-e\cos E}$$

All the expressions for the partial derivatives of the  $R_n$  terms can be found in Table B.1.

Table B.1. DEVELOPMENT OF TERMS FOR  $\hat{H}$ .

$\frac{\partial R_1}{\partial i} = s\omega s\Omega siH_4 - s\omega c\Omega siH_5 + s\omega ciH_6$	$\frac{\partial R_2}{\partial i} = c\omega s\Omega siH_4 - c\omega c\Omega siH_5 + c\omega ciH_6$
$\frac{\partial R_1}{\partial \Omega} = -P_4H_4 + P_1H_5$	$\frac{\partial R_2}{\partial \Omega} = -P_5H_4 + P_2H_5$
$\frac{\partial R_1}{\partial \omega} = P_2H_4 + P_5H_5 + P_8H_6$	$\frac{\partial R_2}{\partial \omega} = -P_1H_4 - P_4H_5 - P_7H_6$
$\frac{\partial R_4}{\partial i} = s\omega s\Omega siH_7 - s\omega c\Omega siH_8 + s\omega ciH_9$	$\frac{\partial R_5}{\partial i} = c\omega s\Omega siH_7 - c\omega c\Omega siH_8 + c\omega ciH_9$
$\frac{\partial R_4}{\partial \Omega} = -P_4H_7 + P_1H_8$	$\frac{\partial R_5}{\partial \Omega} = -P_5H_7 + P_2H_8$
$\frac{\partial R_4}{\partial \omega} = P_2H_7 + P_5H_8 + P_8H_9$	$\frac{\partial R_5}{\partial \omega} = -P_1H_7 - P_4H_8 - P_7H_9$
$\frac{\partial R_7}{\partial i} = s\omega s\Omega siH_1 - s\omega c\Omega siH_2 + s\omega ciH_3$	$\frac{\partial R_8}{\partial i} = c\omega s\Omega siH_1 - c\omega c\Omega siH_2 + c\omega ciH_3$
$\frac{\partial R_7}{\partial \Omega} = -P_4H_1 + P_1H_2$	$\frac{\partial R_8}{\partial \Omega} = -P_5H_1 + P_2H_2$
$\frac{\partial R_7}{\partial \omega} = P_2H_1 + P_5H_2 + P_8H_3$	$\frac{\partial R_8}{\partial \omega} = -P_1H_1 - P_4H_2 - P_7H_3$

## APPENDIX C

### FILTER CODE (MATLAB)

Following is the Matlab code for the extended Kalman filter described in this paper. This particular filter models the 2-body orbital dynamics problem, including secular and periodic perturbations. It requires 2 data files for input (see header of filter code):

*datain* - contains a time-tagged initial orbital element set and an unspecified number of time-tagged pairs of direction cosines and corresponding receiving sites

*siteinfo* - contains pertinent information about the set of receiver sites comprising the radar plane detection system.

The filter calls 3 functions:

*enewton* - performs a Newton-Rapson iteration to obtain eccentric anomaly, given a mean anomaly and eccentricity

*intper* - performs a Newton-Rapson iteration to propagate satellite position to an in-radar-plane condition.

*twopi* - forces angular measurements to a number between 0 and  $2\pi$ .

### Extended Kalman Estimator

The code for these functions follows the filter code.

```
%*****
                                This estimator requires 2 input files to run
DATAIN & SITEINFO.
    datain=[250  116  82  191626.933  0  0
    103.591322  .00756997  66.81264  189.71773  26.77689
116.53101
    83  65024.876  6  14.839  .092  0
    83  83436.223  5  -76.912  .012  0
```

```

83 83436.259 4 -63.554 .009 0
83 83436.397 1 58.982 .062 0
83 83436.408 3 -57.058 .043 0
83 83436.425 6 -78.987 .034 0
83 160057.722 6 64.179 .030 0
83 174304.847 3 -16.315 .020 0
83 174304.904 5 -58.495 .007 0
83 174304.906 6 -62.516 -.001 0
83 174304.908 1 74.290 .012 0];

```

```

siteinfo=[1 32.57840 -116.97016 1.87473e-5 8.58120
2 33.44600 -106.99824 2.212449e-4 3.13900
3 33.33239 -93.55039 8.143107e-6 -4.27563
4 33.14672 -91.02096 6.738134e-7 -5.66895
5 32.28768 -83.53628 1.118243e-5 -9.71924
6 32.04323 -81.92609 3.866064e-6 -10.5800]

```

```

%*****
function[xkeep,Tkeep,Tint,delTint,resid,xint,Pkeep]=...
orbper(datain,siteinfo);

```

```

inpels=[datain(1,:)';datain(2,:)'];
observ=datain(3:length(datain(:,1)),1:5);
K=inpels(1);

```

```

for i=1:7
lat(i)=siteinfo(i,2)*pi/180;
lon(i)=siteinfo(i,3)*pi/180;
alt(i)=siteinfo(i,4);
az(i)=siteinfo(i,5)*pi/180;
end

```

```

%*****
THIS PROGRAM PROPAGATES A SATELLITE ORBIT AS A 2-BODY PROBLEM
WITH SECULAR VARIATIONS IN OMEGA, omega, and MEAN ANOMALY. IT
CALLS THE FOLLOWING FUNCTIONS:

```

TWOPI - places angle between 0 & 2\*pi.

INTSEC - iterates to an in-fence-plane condition when a fence plane crossing is detected.

ENEWTON - solves for eccentric anomaly, given values for mean anomaly and eccentricity.

```

%*****
* DEFINE EARTH ROTATION RATE *

```

```

%*****
earthrot=.05883378171654; % Define earth rotation rate (rad/TU).
J2=1.082645e-3;

```

```

%*****
* DEFINE VARIOUS TERMS *

```

```

%*****
R=[4e-8 0;0 4e-8]; % Measurement noise matrix.

```

```

Pkkml=eye(6)*1e-8; % Initialize error covariance matrix.
Pkeep(:,1:6)=Pkkml;
resid(:,1)=[0;0];
G=zeros(6,2); % Initialize Kalman gain.
finc=33.58310*pi/180; % Define fence inclination.
cosfinc=cos(finc);
sinfinc=sin(finc);
lonx=-101.31348*pi/180; % Define location of fence x-axis.
%*****
* INITIALIZE STATES (ORBITAL ELEMENTS) *
%*****
xnow=[(inpels(7)/(2*pi*13.44689317))^(2/3);
      inpels(8);inpels(9:12).*pi/180];
xkeep(:,1)=xnow; % Save original states.
%*****
* CALCULATE INITIAL ECCENTRIC ANOMALY *
%*****
EA(1)=Enewton(xnow(6),xnow(6),xnow(2));
%*****
* FIND INITIAL r and TA *
%*****
costA=(cos(EA(1))-xnow(2))/(1-xnow(2)*cos(EA(1)));
sinTA=sqrt(1-xnow(2)^2)*sin(EA(1))/(1-xnow(2)*cos(EA(1)));
r=xnow(1)*(1-xnow(2)^2)/(1+xnow(2)*costA);
TA(1)=twopi(asin(sinTA));
if TA(1)<pi
    if costA<0
        TA(1)=pi-TA(1); % Perform quadrant check
    end % for true anomaly.
else
    if costA<0
        TA(1)=3*pi-TA(1);
    end
end

%*****
* CALCULATE TRANSFORMATION MATRIX (ORBITAL TO INERTIAL) *
%*****
cosperi=cos(xnow(5));
sinperi=sin(xnow(5));
cosascnd=cos(xnow(4)); % Calculate sines & cosines of
sinascnd=sin(xnow(4)); % angular orbital elements.
costilt=cos(xnow(3));
sintilt=sin(xnow(3));

P1=cosperi*cosascnd-sinperi*sinascnd*costilt;
P2=-sinperi*cosascnd-cosperi*sinascnd*costilt;
P4=cosperi*sinascnd+sinperi*cosascnd*costilt;

```

```

P5=-sinperi*sinascnd+cosperi*cosascnd*costilt;
P7=sinperi*sintilt;
P8=cosperi*sintilt;
%*****
*   INITIALIZE TIME   *
%*****
oneJan92=98.920250931*pi/180;
TUpperday=107.0879334097483;
secperTU=806.81359;
JD=inpels(3);
time=inpels(4);
hrs=fix(time*1e-4);
min=fix(rem(time,1e4)*1e-2);
sec=rem(time,1e2);
Tfilter=(hrs*3600+min*60+sec)/secperTU;
Tgnwch=rem(earthrot*TUpperday*(Tfilter/TUpperday+...
          (JD-1))+oneJan92,2*pi)/earthrot;
Told=Tfilter;
Tkeep(1)=JD+Tfilter*secperTU/86400;      % Save original time

%*****
*   INITIALIZE TIME OF FIRST OBSERVATION   *
%*****

time=observ(1,2);
hrs=fix(time*1e-4);
min=fix(rem(time,1e4)*1e-2);
sec=rem(time,1e2);
timeobs=(hrs*3600+min*60+sec)/secperTU;
%*****
*   CALCULATE OUT-OF-FENCE-PLANE COORDINATE OF SATELLITE POSITION   *
%*****
theta=twopi(earthrot*Tgnwch+lonx);
sintheta=sin(theta);
costheta=cos(theta);
zfence=.0031+(-sinfinc*costheta*P1...
             -sinfinc*sintheta*P4...
             +cosfinc*P7)*r*cosTA... % Calculate current magnitude
             +(-sinfinc*costheta*P2...% of out-of-plane coordinate.
             -sinfinc*sintheta*P5...
             +cosfinc*P8)*r*sinTA;

%*****
*   PROPAGATE ORBITAL ELEMENTS TO NEXT FENCE-PLANE INTERSECTION   *
%*****
J2=1.082645e-3;
p=1;

```

```

n=0;
for k=1:K
    Tloop=pi/8*xnow(1)^1.5;
%*****
%   INCREMENT MEAN ANOMALY & APPLY SECULAR VARIATION   *
%*****
    mnmotion=xnow(1)^(-3/2);
    xnow(6)=twopi(xnow(6)+mnmotion*Tloop);
    EA(k+1)=enewton(xnow(6),xnow(6),xnow(2));
    costA=(cos(EA(k+1))-xnow(2))/(1-xnow(2)*cos(EA(k+1)));
    sinTA=sqrt(1-xnow(2)^2)*sin(EA(k+1))/(1-xnow(2)*cos(EA(k+1)));
    r=xnow(1)*(1-xnow(2)^2)/(1+xnow(2)*costA);

    TA(k+1)=twopi(asin(sinTA));
    if TA(k+1)<pi
        if costA<0
            TA(k+1)=pi-TA(k+1);           % Perform quadrant check
        end                               %   for true anomaly.
    else
        if costA<0
            TA(k+1)=3*pi-TA(k+1);
        end
    end
%*****
%   APPLY SECULAR VARIATIONS TO omega & OMEGA   *
%*****
    delTasec=twopi(TA(k+1)-TA(k));
    semilat=xnow(1)*(1-xnow(2)^2);
    Q1=-3*J2/semilat^2;
    SOMEGA=Q1*cos(xnow(3))/2;
    Somega=(-Q1)*(2-5/2*sin(xnow(3))^2)/2;
    delsOMEGA=SOMEGA*delTasec;
    delsomega=Somega*delTasec;
    xnow(4)=xnow(4)+delsOMEGA;
    xnow(5)=xnow(5)+delsomega;
%*****
%   CALCULATE ATMOSPHERIC DENSITY   *
%*****
    k2=3e-6;
    k3=21/6378.135;
    atmdens=k2*exp((1-r)/k3);
%*****
%   APPLY DRAG PERTURBATIONS TO a & e   *
%*****
    k1=-4*6378.135;
    delldrag=[k1*xnow(1)^2*(1+xnow(2))*atmdens*delTasec;
              k1*xnow(1)*(1-xnow(2)^2)*atmdens*delTasec;
              0;0;0;0];

```

```

xnow=xnow+deldrag;
% *****
*   CALCULATE TRANSFORMATION MATRIX (ORBITAL TO INERTIAL)   *
% *****
cosperi=cos(xnow(5));
sinperi=sin(xnow(5));
cosascnd=cos(xnow(4));           % Calculate sines & cosines of
sinascnd=sin(xnow(4));           % angular orbital elements.
costilt=cos(xnow(3));
sintilt=sin(xnow(3));

P1=cosperi*cosascnd-sinperi*sinascnd*costilt;
P2=-sinperi*cosascnd-cosperi*sinascnd*costilt;
P4=cosperi*sinascnd+sinperi*cosascnd*costilt;
P5=-sinperi*sinascnd+cosperi*cosascnd*costilt;
P7=sinperi*sintilt;
P8=cosperi*sintilt;
% *****
*   UPDATE TIME   *
% *****
Tgnwch=Tgnwch+Tloop;
Tfilter=Tfilter+Tloop;
% *****
* CALCULATE OUT-OF-FENCE-PLANE COORDINATE OF SATELLITE POSITION *
% *****
theta(k+1)=twopi(earthrot*Tgnwch+lonx);
sintheta=sin(theta(k+1));
costheta=cos(theta(k+1));
zfold=zfence;
zfence=.0031+(-sinfinc*costheta*P1...
            -sinfinc*sintheta*P4...
            +cosfinc*P7)*r*cosTA... % Calculate current magnitude
            +(-sinfinc*costheta*P2... % of out-of-plane coordinate.
            -sinfinc*sintheta*P5...
            +cosfinc*P8)*r*sinTA;
% *****
*   CHECK FOR FENCE PLANE INTERSECTION   *
% *****
*   NEGATIVE TO POSITIVE ??   *
% *****
if zfence>0
    if zfold<0
        n=n+1;
        negtopos=n;
        xnow=xnow';
        [Tloop,Tfilter,Tgnwch,flag,xnow,r,cosTA,...
         sinTA,TA(k+1),theta(k+1),EA(k+1),zfence]=...

```

```

        inttemp(xnow,r,cosTA,...
        sinTA,TA(k+1),theta(k+1),EA(k+1),P1,P2,P4,...
        P5,P7,P8,Tgnwch,Tfilter,Tloop);
    xnow=xnow';
end
end
%*****
* POSITIVE TO NEGATIVE ?? *
%*****
if zfence<0
    if zfold>0
        n=n+1;
        postoneg=n;
        xnow=xnow';
        [Tloop,Tfilter,Tgnwch,flag,xnow,r,cosTA,...
        sinTA,TA(k+1),theta(k+1),EA(k+1),zfence]=...
        inttemp(xnow,r,cosTA,...
        sinTA,TA(k+1),theta(k+1),EA(k+1),P1,P2,P4,...
        P5,P7,P8,Tgnwch,Tfilter,Tloop);
        xnow=xnow';
    end
end

TAold=TA(k+1);
%*****
* SATELLITE IN NAVSPASUR WINDOW ?? *
%*****

if flag==1

%*****
* CALCULATE TIME FROM LAST FILTER UPDATE (LAST OBS) *
%*****

    delobs=timeobs-Tfilter;
    while abs(delobs)<1
        if length(observ(:,1))>=p
            delobs=timeobs-Tfilter;

            delT=delobs;
            delTint(p)=delT*secperTU;
            Tint(p)=(timeobs*secperTU)/3600;

            Tupdate=timeobs-Told;
            if Tupdate<0
                Tupdate=Tupdate+Tuperday;
            end
            Told=timeobs;

```

```

Tfilter=Tfilter+deltT;
Tgnwch=Tgnwch+deltT;

%*****
*   INCORPORATE PERIODIC VARIATIONS   *
%*****
    xmean=xnow;
    daper=3*J2*xnow(1)/(2*semilat^2*(1-xnow(2)^2))*...
        sin(xnow(3))^2*cos(2*(xnow(5)+TA(k+1)));
    deper=3*J2/(2*semilat^2)*((1-3/2*sin(xnow(3))^2)*cosTA+...
        1/4*sin(xnow(3))^2*cos(2*xnow(5)+TA(k+1))+...
        7/12*sin(xnow(3))^2*cos(2*xnow(5)+3*TA(k+1)));
    diper=-3*J2/(8*semilat^2)*sin(2*xnow(3))*...
        cos(2*(xnow(5)+TA(k+1)));
    dOMper=3*J2/(4*semilat^2)*cos(xnow(3))*...
        sin(2*(xnow(5)+TA(k+1)));
    dnewper=-3*J2/(4*semilat^2)*(1-5/2*sin(xnow(3))^2)*...
        sin(2*(xnow(5)+TA(k+1)));
    dtemp=3*J2/(2*semilat^2)*(1/xnow(2))*...
        (1-3/2*sin(xnow(3))^2)*sinTA-...
        1/4*sin(xnow(3))^2*sin(2*xnow(5)+TA(k+1))+...
        7/12*sin(xnow(3))^2*sin(2*xnow(5)+3*TA(k+1))+...
        1/2*((1-3/2*sin(xnow(3))^2)*sin(2*TA(k+1))-...
        (1-5/2*sin(xnow(3))^2)*sin(2*(xnow(5)+TA(k+1)))+...
        3/8*sin(xnow(3))^2*sin(2*xnow(5)+4*TA(k+1)));
    domper=dtemp;
    dMAper=dnewper-domper;
    varper=[daper;deper;diper;dOMper;domper;dMAper];
    xnow=xnow+varper; xnow(6)=twopi(xnow(6));
    EA(k+1)=enewton(xnow(6),xnow(6),xnow(2));
    cosTA=(cos(EA(k+1))-xnow(2))/(1-xnow(2)*cos(EA(k+1)));
    sinTA=sqrt(1-xnow(2)^2)*sin(EA(k+1))/(1-xnow(2)*cos(EA(k+1)));
    r=xnow(1)*(1-xnow(2)^2)/(1+xnow(2)*cosTA);

    TA(k+1)=twopi(asin(sinTA));
    if TA(k+1)<pi
        if cosTA<0
            TA(k+1)=pi-TA(k+1);           % Perform quadrant check
        end                               %   for true anomaly.
    else
        if cosTA<0
            TA(k+1)=3*pi-TA(k+1);
        end
    end

%*****
*   CALCULATE ANGULAR DISPLACEMENT OF RECEIVER SITE FROM I-AXIS   *
%*****

```

```

phi=twopi (earthrot*Tgnwch+lon (observ (p, 3) ));
sinphi=sin (phi) ;

sinlat=sin (lat (observ (p, 3) ));
coslat=cos (lat (observ (p, 3) ));
sinlon=sin (lon (observ (p, 3) ));
coslon=cos (lon (observ (p, 3) ));
cosperi=cos (xnow (5) );
sinperi=sin (xnow (5) );
cosascnd=cos (xnow (4) );
sinascnd=sin (xnow (4) );
costilt=cos (xnow (3) );
sintilt=sin (xnow (3) );

P1=cosperi*cosascnd-sinperi*sinascnd*costilt;
P2=-sinperi*cosascnd-cosperi*sinascnd*costilt;
P4=cosperi*sinascnd+sinperi*cosascnd*costilt;
P5=-sinperi*sinascnd+cosperi*cosascnd*costilt;
P7=sinperi*sintilt;
P8=cosperi*sintilt;

    sinaz=sin (az (observ (p, 3) ));
    cosaz=cos (az (observ (p, 3) ));

    H1=coslat*cosphi;
    H2=coslat*sinphi;
    H3=sinlat;
    H4=-sinphi*cosaz-sinlat*cosphi*sinaz;
    H5=cosaz*cosphi-sinaz*sinlat*sinphi;
    H6=sinaz*coslat;
    H7=sinaz*sinphi-cosaz*sinlat*cosphi;
    H8=-sinaz*cosphi-cosaz*sinlat*sinphi;
    H9=cosaz*coslat;

    R1=H4*P1+H5*P4+H6*P7;
    R2=H4*P2+H5*P5+H6*P8;
    R4=H7*P1+H8*P4+H9*P7;
    R5=H7*P2+H8*P5+H9*P8;
    R7=H1*P1+H2*P4+H3*P7;
    R8=H1*P2+H2*P5+H3*P8;

```

\*\*\*\*\*

```

* ESTIMATE MEASUREMENT *
%*****
Rsite=sqrt(1-(2-1/298.26)/298.26*sinlat^2)+alt(observ(p,3));
roffset=.0031;
rhoH=r*(R7*cosTA+R8*sinTA)-Rsite;

rhoE=r*(R1*cosTA+R2*sinTA);

rhoN=r*(R4*cosTA+R5*sinTA)+roffset;

rho=sqrt(rhoH^2+rhoE^2+rhoN^2);

zest(:,p)=[rhoE/rho;rhoN/rho];

size=xnow(1);shape=xnow(2);tilt=xnow(3);
ascnd=xnow(4);peri=xnow(5);MA=xnow(6);
%*****
* CALCULATE COVARIANCE MATRIX P *
%*****
J2=1.082645e-3;
sinEA=sin(EA(k+1));
cosEA=cos(EA(k+1));
sindecl=sintilt*sin(TA(k+1)+peri);
semilat=size*(1-shape^2);
%*****
* CALCULATE APPROXIMATE delta(TRUE ANOMALY) *
%*****
mnmotion=xnow(1)^(-3/2);
delMA=mnmotion*Tupdate;
delTA=delMA;
Alphi=-(1+shape^2)*sinEA+2*shape*sinEA*cosEA;
A2phi=1-shape*cosEA;
A3phi=2-5/2*sintilt^2;
A4phi=1-3*sindecl^2;
A5phi=1-shape^2;
A6phi=sqrt(1/size+J2/r^3*A4phi);
A7phi=1+shape*cosTA;

dOMEGAda=3*J2/(size*semilat^2)*costilt*delTA;

dOMEGAd=-6*J2*size*shape/semilat^3*costilt*delTA;

dOMEGAdi=3*J2/(2*semilat^2)*sintilt*delTA;

dOMEGAdM=-3*J2/(size*semilat^2)*costilt*Alphi/(sinTA*A2phi^3);

domegada=-3*J2/(size*semilat^2)*A3phi*delTA;
domegade=6*J2*size*shape/semilat^3*A3phi*delTA;

```

```

domegadi=-15*J2/(2*semilat^2)*sintilt*costilt*delTA;
domegadM=-3*J2/(2*semilat^2)*A3phi*Alphi/(sinTA*A2phi^3);

drkdak=A5phi/A7phi;
dMAda=3/2*Tupdate*A6phi*(-1/size^2+J2*A4phi*(-3/r^4)*drkdak);
drkdek=(-2*size*shape*(1-shape*cosTA)-semilat*cosTA)/A7phi^2;
dMAde=3/2*Tupdate*A6phi*J2*A4phi*(-3/r^4)*drkdek;
dsindkdi=sin(TA(k+1)+peri)*costilt;
dMAdi=3*Tupdate*A6phi*(-3*J2/r^3)*sindecl*dsindkdi;
dsindkdo=sintilt*cos(TA(k+1)+peri);
dMAadomega=3*Tupdate*A6phi*(-3*J2/r^3)*sindecl*dsindkdo;
drdTA=semilat*shape*sinTA/A7phi^2;
dsinddTAd=dsindkdo;
dmessdTAd=-3*J2/r^2*drdTA-(-9*J2/r^4*sindecl^2*drdTA+...
        6*J2/r^3*sindecl*dsinddTAd);
dTAdMA=-Alphi/(sinTA*A2phi^3);
dMAadM=1+3/2*Tupdate*A6phi*dmessdTAd*dTAdMA;

dada=1+2*k1*size*(1+shape)*atmdens*delTA;
dade=k1*size^2*atmdens*delTA;
dadM=-k1*size^2*(1+shape)*atmdens*dTAdMA;

deda=k1*A5phi*atmdens*delTA;
dede=1-2*k1*size*shape*atmdens*delTA;
dedM=-k1*size*A5phi*atmdens*dTAdMA;

phimat=[dada dade 0 0 0 dadM;
        deda dede 0 0 0 dedM;
        0 0 1 0 0 0;
        dOMEGAda dOMEGAd dOMEGAdi 1 0 dOMEGAdM;
        domegada domegade domegadi 0 1 domegadM;
        dMAda dMAde dMAdi 0 dMAadomega dMAadM];

%*****
%  CALCULATE PLANT NOISE  *
%*****
J2=1.0826e-3;
semilat=xnow(1)*(1-xnow(2)^2);
siga2=(3*J2*xnow(1)/(2*semilat^2*(1-xnow(2)^2))*...
        sin(xnow(3))^2*cos(2*(xnow(5)+TA(k+1))))^2;
sige2=(3*J2/(2*semilat^2)*((1-3/2*sin(xnow(3))^2)*cosTA+...
        sin(2*xnow(3))*cos(2*(xnow(5)+TA(k+1))))^2;
sigi2=(3*J2/(8*semilat^2)*sin(2*xnow(3))*...
        cos(2*(xnow(5)+TA(k+1))))^2;
mnmotion=xnow(1)^(-3/2);
MApert=mnmotion*3*J2/(2*semilat^2)*(1-3/2*sin(xnow(3))^2)*...
        sqrt(1-xnow(2)^2);
sigOMEG2=(3*J2/(2*semilat^2)*mnmotion*cos(xnow(3))*Tupdate)^2;
sigomeg2=(3*J2/(2*semilat^2)*mnmotion*...

```

```

        (2-5/2*sin(xnow(3))^2)*Tupdate)^2;
sigMA2=(MApert*Tupdate)^2;
Q=[1e-2*sig2 0 0 0 0 0
   0 1e-3*sige2 0 0 0 0
   0 0 sigi2 0 0 0
   0 0 0 sigOMEG2 0 0
   0 0 0 0 sigomeg2 0
   0 0 0 0 0 sigMA2].*1e-3;

%*****
*   PROPAGATE ERROR COVARIANCE   *
%*****
        Pkk=Pkkml;
        Pkkml=phimat*Pkk*phimat'+Q;
%*****
*   CALL IN OBSERVATION DATA   *
%*****
        cosalpha=sin(observ(p,4)*pi/180);
        cosbeta=sin(observ(p,5)*pi/180);
        z(:,p)=[cosalpha;cosbeta];
%*****
*   CALCULATE LINEARIZED MEASUREMENT MATRIX H   *
%*****
        a1=1-xnow(2)^2;
        a2=1+xnow(2)*costA;
        a3=2*xnow(2)+costA*(1+xnow(2)^2);
        a4=2*xnow(2)*sinEA*cosEA;
        a5=1+xnow(2)^2;
        a6=-a5*sinEA+a4;
        a7=1-xnow(2)*cosEA;

        drda=a1/a2;
        drde=-xnow(1)*a3/a2^2;

        dcostAdT=-sinTA;
        dTAdEA=(-a5*sinEA+a4)/(-sinTA*a7^2);
        dEAdMA=1/a7;
        dcostAdM=dcostAdT*dTAdEA*dEAdMA;

        dsinTAdT=costA;
        dsinTAdM=dsinTAdT*dTAdEA*dEAdMA;

        drdTAdT=xnow(1)*xnow(2)*a1*sinTA/a2^2;
        drdMA=drdTAdT*dTAdEA*dEAdMA;

        dRldi=sinperi*sinascnd*sintilt*H4-...
               sinperi*cosascnd*sintilt*H5+...
               sinperi*costilt*H6;

```

```

dR2di=cosperi*sinascnd*sintilt*H4-...
      cosperi*cosascnd*sintilt*H5+...
      cosperi*costilt*H6;
dR4di=sinperi*sinascnd*sintilt*H7-...
      sinperi*cosascnd*sintilt*H8+...
      sinperi*costilt*H9;
dR5di=cosperi*sinascnd*sintilt*H7-...
      cosperi*cosascnd*sintilt*H8+...
      cosperi*costilt*H9;
dR7di=sinperi*sinascnd*sintilt*H1-...
      sinperi*cosascnd*sintilt*H2+...
      sinperi*costilt*H3;
dR8di=cosperi*sinascnd*sintilt*H1-...
      cosperi*cosascnd*sintilt*H2+...
      cosperi*costilt*H3;

dR1dOM=-P4*H4+P1*H5;
dR2dOM=-P5*H4+P2*H5;
dR4dOM=-P4*H7+P1*H8;
dR5dOM=-P5*H7+P2*H8;
dR7dOM=-P4*H1+P1*H2;
dR8dOM=-P5*H1+P2*H2;

dR1dom=P2*H4+P5*H5+P8*H6;
dR2dom=-P1*H4-P4*H5-P7*H6;
dR4dom=P2*H7+P5*H8+P8*H9;
dR5dom=-P1*H7-P4*H8-P7*H9;
dR7dom=P2*H1+P5*H2+P8*H3;
dR8dom=-P1*H1-P4*H2-P7*H3;

dpHda=(R7*cosTA+R8*sinTA)*drda;
dpEda=(R1*cosTA+R2*sinTA)*drda;
dpNda=(R4*cosTA+R5*sinTA)*drda;
dpda=(rhoH*dpHda+rhoE*dpEda+rhoN*dpNda)/rho;

dpHde=(R7*cosTA+R8*sinTA)*drde;
dpEde=(R1*cosTA+R2*sinTA)*drde;
dpNde=(R4*cosTA+R5*sinTA)*drde;
dpde=(rhoH*dpHde+rhoE*dpEde+rhoN*dpNde)/rho;

dpHdi=(dR7di*cosTA+dR8di*sinTA)*r;
dpEdi=(dR1di*cosTA+dR2di*sinTA)*r;
dpNdi=(dR4di*cosTA+dR5di*sinTA)*r;
dpdi=(rhoH*dpHdi+rhoE*dpEdi+rhoN*dpNdi)/rho;

dpHdOM=(dR7dOM*cosTA+dR8dOM*sinTA)*r;
dpEdOM=(dR1dOM*cosTA+dR2dOM*sinTA)*r;

```

```

dpNdOM=(dR4dOM*cosTA+dR5dOM*sinTA)*r;
dpdOM=(rhoH*dpHdOM+rhoE*dpEdOM+rhoN*dpNdOM)/rho;

dpHdom=(dR7dom*cosTA+dR8dom*sinTA)*r;
dpEdom=(dR1dom*cosTA+dR2dom*sinTA)*r;
dpNdom=(dR4dom*cosTA+dR5dom*sinTA)*r;
dpdOM=(rhoH*dpHdom+rhoE*dpEdom+rhoN*dpNdom)/rho;

dpHdMA=(R7*dcosTAdM+R8*dsinTAdM)*r+(R7*cosTA+R8*
sinTA)*drdMA;
dpEdMA=(R1*dcosTAdM+R2*dsinTAdM)*r+(R1*cosTA+R2*
sinTA)*drdMA;
dpNdMA=(R4*dcosTAdM+R5*dsinTAdM)*r+(R4*cosTA+R5*
sinTA)*drdMA;
dpdMA=(rhoH*dpHdMA+rhoE*dpEdMA+rhoN*dpNdMA)/rho;

drhoEda=dpEda/rho-rhoE*dpda/rho^2;
drhoNda=dpNda/rho-rhoN*dpda/rho^2;

drhoEde=dpEde/rho-rhoE*dpde/rho^2;
drhoNde=dpNde/rho-rhoN*dpde/rho^2;

drhoEdi=dpEdi/rho-rhoE*dpdi/rho^2;
drhoNdi=dpNdi/rho-rhoN*dpdi/rho^2;

drhoEdOM=dpEdOM/rho-rhoE*dpdOM/rho^2;
drhoNdOM=dpNdOM/rho-rhoN*dpdOM/rho^2;

drhoEdom=dpEdom/rho-rhoE*dpdom/rho^2;
drhoNdom=dpNdom/rho-rhoN*dpdom/rho^2;

drhoEdMA=dpEdMA/rho-rhoE*dpdMA/rho^2;
drhoNdMA=dpNdMA/rho-rhoN*dpdMA/rho^2;

H=[drhoEda drhoEde drhoEdi drhoEdOM drhoEdom drhoEdMA;
drhoNda drhoNde drhoNdi drhoNdOM drhoNdom drhoNdMA];
%*****
* CALCULATE KALMAN GAIN *
%*****

G=Pkkml*H'*inv(H*Pkkml*H'+R);
resid(:,p)=z(:,p)-zest(:,p);

%*****
* CALCULATE IMPROVED COVARIANCE *
%*****
Pkk=(eye(6)-G*H)*Pkkml;

```

```

Pkeep(:,p*6+1:6*(p+1))=Pkk;
%*****
% * CALCULATE IMPROVED MEAN ORBITAL ELEMENTS *
%*****
    xnow=xmean;
    G*resid(:,p);
    xnow=xnow+G*resid(:,p);
    xnow(6)=twopi(xnow(6));

    xint(1:2,p)=xnow(1:2);
    xint(3:6,p)=xnow(3:6)*180/pi;
%*****
% * CALCULATE IMPROVED ECCENTRIC ANOMALY *
%*****
    EA(k+1)=enewton(xnow(6),xnow(6),xnow(2));
%*****
% * SOLVE FOR IMPROVED cos(TA), sin(TA), r, sin(decl), n *
%*****
    cosTA=(cos(EA(k+1))-xnow(2))/(1-xnow(2)*cos(EA(k+1)));
    sinTA=sqrt(1-xnow(2)^2)*sin(EA(k+1))/(1-xnow(2)...
        *cos(EA(k+1)));
    r=xnow(1)*(1-xnow(2)^2)/(1+xnow(2)*cosTA);

    TA(k+1)=twopi(asin(sinTA));
    if TA(k+1)<pi
        if cosTA<0
            TA(k+1)=pi-TA(k+1);           % Perform quadrant check
        end                               % for true anomaly.
    else
        if cosTA<0
            TA(k+1)=3*pi-TA(k+1);
        end
    end

    TAold=TA(k+1);

%*****
%*****
    if length(observ(:,1))>p
        p=p+1;
        time=observ(p,2);
        hrs=fix(time*1e-4);
        min=fix(rem(time,1e4)*1e-2);
        sec=rem(time,1e2);
        timeobs=(hrs*3600+min*60+sec)/secperTU;
        delobs=timeobs-Tfilter;
    else
        delobs=2;
    end

```

```

        end
    end
end
end
flag=0;

```

```

%*****
*   RESET TIMES FOR NEW DAY   *
%*****
    if Tgnwch>106.7955369153698
        Tgnwch=Tgnwch-106.7955369153698;
    end
    if Tfilter>107.0879334
        Tfilter=Tfilter-107.0879334;
        JD=JD+1;
    end
    xkeep(:,k+1)=xnow;
    Tkeep(k+1)=JD+Tfilter*secperTU/86400;
end

```

### In-plane Iteration

```

function[T,Tfilter,Tgnwch,flag,xnow,r,cosTA,...
        sinTA,TA,theta,Enow,zfence]=...
        inttemp(xnow,r,cosTA,sinTA,TA,theta,Enow,...
        P1,P2,P4,P5,P7,P8,Tgnwch,Tfilter,T);
xnow=xnow';
J2=1.082645e-3;
earthrot=.05883378171654;%Define earth rotation rate(rad/TU).
lonx=-101.31348*pi/180;
finc=33.58310*pi/180;
sinfinc=sin(finc);
cosfinc=cos(finc);
delt=0;
zfence=1; % INITIALIZE OUT-OF-FENCE-PLANE VALUE OF POSITION
%*****
%           *   ITERATE TO IN-PLANE CONDITION   *
%*****
    while abs(zfence)>=1e-8
%*****
%           *   ADD IN PERIODIC VARIATIONS   *
%*****
        semilat=xnow(1)*(1-xnow(2)^2);
        daper=3*J2*xnow(1)/(2*semilat^2*(1-xnow(2)^2))*...
            sin(xnow(3))^2*cos(2*(xnow(5)+TA));

```

```

deper=3*J2/(2*semilat^2)*((1-3/2*sin(xnow(3))^2)*cosTA+...
    1/4*sin(xnow(3))^2*cos(2*xnow(5)+TA)+...
    7/12*sin(xnow(3))^2*cos(2*xnow(5)+3*TA));
diper=-3*J2/(8*semilat^2)*sin(2*xnow(3))*...
    *cos(2*(xnow(5)+TA));
dOMper=3*J2/(4*semilat^2)*cos(xnow(3))*sin(2*(xnow(5)+TA));
dnewper=-3*J2/(4*semilat^2)*(1-5/2*sin(xnow(3))^2)*...
    *sin(2*(xnow(5)+TA));
dtemp=3*J2/(2*semilat^2)*(1/xnow(2))*...
    ((1-3/2*sin(xnow(3))^2)*sinTA+...
    1/4*sin(xnow(3))^2*sin(2*xnow(5)+TA)+...
    7/12*sin(xnow(3))^2*sin(2*xnow(5)+3*TA))+...
    1/2*((1-3/2*sin(xnow(3))^2)*sin(2*TA)-...
    (1-5/2*sin(xnow(3))^2)*sin(2*(xnow(5)+TA))+...
    3/8*sin(xnow(3))^2*sin(2*xnow(5)+4*TA));
domper=dtemp;
dMAper=dnewper-domper;
varper=[daper;deper;diper;dOMper;domper;dMAper];
xper=xnow+varper;

EAper=ewton(xper(6),xper(6),xper(2));
cosTAper=(cos(EAper)-xper(2))/(1-xper(2)*cos(EAper));
sinTAper=sqrt(1-xper(2)^2)*sin(EAper)/(1-xper(2)*...
    *cos(EAper));
rper=xper(1)*(1-xper(2)^2)/(1+xper(2)*cosTAper);

TAper=twopi(asin(sinTAper));
if TAper<pi
    if costAper<0
        TAper=pi-TAper;           % Perform quadrant check
    end                             % for true anomaly.
else
    if costAper<0
        TAper=3*pi-TAper;
    end
end

%*****
%      *      RECALCULATE PERIODIC TRANSFORMATION MATRIX      *
%*****
P1per=cos(xper(5))*cos(xper(4))-...
    sin(xper(5))*sin(xper(4))*cos(xper(3));
P2per=-sin(xper(5))*cos(xper(4))-...
    cos(xper(5))*sin(xper(4))*cos(xper(3));
P4per=cos(xper(5))*sin(xper(4))+...
    sin(xper(5))*cos(xper(4))*cos(xper(3));
P5per=-sin(xper(5))*sin(xper(4))*...
    +cos(xper(5))*cos(xper(4))*cos(xper(3));

```

```

P7per=sin(xper(5))*sin(xper(3));
P8per=cos(xper(5))*sin(xper(3));
stuff=sinfinc*earthrot*xper(1)^1.5*rper*...
    costAper*(P1per*sin(theta)...
    -P4per*cos(theta))+sinfinc*earthrot*xper(1)^1.5*...
    rper*sinTAper*(P2per*sin(theta)-P5per*...
    cos(theta))+xper(1)/(1-xper(2)*cos(EAper))*...
    (-sin(EAper))*(-sinfinc*P1per*cos(theta)-...
    sinfinc*P4per*sin(theta)+cosfinc*P7per)+...
    sqrt(1-xper(2)^2)*cos(EAper)*(-sinfinc*P2per*...
    cos(theta)-sinfinc*P5per*sin(theta)+cosfinc*P8per));

zfence=.0031+(-sinfinc*cos(theta)*P1per-sinfinc*...
    sin(theta)*P4per+cosfinc*P7per)*rper*...
    costAper+(-sinfinc*cos(theta)*P2per*...
    -sinfinc*sin(theta)*P5per+cosfinc*P8per)*...
    rper*sinTAper;
delMA=-zfence/stuff;
mnmotion=xnow(1)^(-3/2);
del2T=delMA/mnmotion;
%*****
PROPAGATE MEAN ORBITAL ELEMENTS TO ITERATIVE VALUE OF TIME *
%*****
    xnow(6)=twopi(xnow(6)+delMA);
    Enow=enewton(xnow(6),xnow(6),xnow(2));
    TAold=TA;
    costA=(cos(Enow)-xnow(2))/(1-xnow(2)*cos(Enow));
    sinTA=sqrt(1-xnow(2)^2)*sin(Enow)/(1-xnow(2)*...
        cos(Enow));
    r=xnow(1)*(1-xnow(2)^2)/(1+xnow(2)*costA);

    TA=twopi(asin(sinTA));
    if TA<pi
        if costA<0
            TA=pi-TA;           % Perform quadrant check
                                %   for true anomaly.
        end
    else
        if costA<0
            TA=3*pi-TA;
        end
    end
end
%*****
%      *   APPLY SECULAR VARIATIONS TO omega & OMEGA   *
%*****
    delTA=TA-TAold;
    if delTA>pi/2
        delTA=delTA-2*pi;
    end

```

```

        if delTA<-pi/?
            delTA=delTA+2*pi;
        end
        semilat=xnow(1)*(1-xnow(2)^2);
        Q1=-3*J2/semilat^2;

        SOMEGA=Q1*cos(xnow(3))/2;
        Somega=-Q1*(2-5/2*sin(xnow(3))^2)/2;
        delsOMEGA=SOMEGA*delTA;
        delsomega=Somega*delTA;
        xnow(4)=xnow(4)+delsOMEGA;
        xnow(5)=xnow(5)+delsomega;
%*****
%      *   CALCULATE ATMOSPHERIC DENSITY   *
%*****
        k2=3e-6;
        k3=21/6378.135;
        atmdens=k2*exp((1-r)/k3);
%*****
%      *   APPLY DRAG PERTURPATIONS TO a & e   *
%*****
        k1=-4*6378.135;
        deldrag=[k1*xr      (1)^2*(1+xnow(2))*atmdens*delTAsec;
                k1*xnow(1)*(1-xnow(2)^2)*atmdens*delTAsec;
                0;0;0;0];
        xnow=xnow+deldrag;
%*****
%      *   RECALCULATE TRANSFORMATION MATRIX (ORBITAL TO INERTIAL)   *
%*****
        P1=cos(xnow(5))*cos(xnow(4))-...
            sin(xnow(5))*sin(xnow(4))*cos(xnow(3));
        P2=-sin(xnow(5))*cos(xnow(4))-...
            cos(xnow(5))*sin(xnow(4))*cos(xnow(3));
        P4=cos(xnow(5))*sin(xnow(4))+...
            sin(xnow(5))*cos(xnow(4))*cos(xnow(3));
        P5=-sin(xnow(5))*sin(xnow(4))+...
            cos(xnow(5))*cos(xnow(4))*cos(xnow(3));
        P7=sin(xnow(5))*sin(xnow(3));
        P8=cos(xnow(5))*sin(xnow(3));
%*****
%      *   IMPLEMENT TIME CORRECTION   *
%*****
        delT=delT+del2T;
        theta=twopi(earthrot*(Tgnwch+delT)+lonx);
    end
%*****
%      *   UPDATE ACTUAL TIME OF INTERSECTION   *
%*****

```

```

Tgnwch=Tgnwch+deltT;
Tfilter=Tfilter+deltT;
T=T+deltT;
xnow=xnow';

```

```

%*****
%      *      CALCULATE FENCE-PLANE COORDINATES      *
%*****
x=(cosfinc*cos(theta)*P1+cosfinc*sin(theta)*P4+...
   sinfinc*P7)*r*cosTA+(cosfinc*cos(theta)*P2+...
   cosfinc*sin(theta)*P5+sinfinc*P8)*r*sinTA;
y=(-sin(theta)*P1+cos(theta)*P4)*r*cosTA...
   +(-sin(theta)*P2+cos(theta)*P5)*r*sinTA;
%*****
DETERMINE WHETHER ANY RCVR MAY BE ABLE TO OBSERVE SATELLITE *
%*****
   if x/sqrt(x^2+y^2)>=cos(40*pi/180)
       flag=1 ;
   end
   zfence=0;

```

### Eccentric Anomaly Iteration

```

function [EA]=Enewton(EA,MA,e)

if MA<EA
    if EA>1.5*pi
        MA=MA+2*pi;
    end
end
errE=1;
while abs(errE)>=1e-10
    errE=EA-e*sin(EA)-MA;
    delEA=(-1/(1-e*cos(EA)))*errE;
    EA=twopi(EA+delEA);
    MA=twopi(MA);
end

```

## Angle Between 0 & $2\pi$

% This function will take any angle (in radians) and  
calculate

% its equivalent between zero and  $2\pi$

function phi=twopi(phi)

```
if phi>=2*pi
    while phi>=2*pi
        phi=phi-2*pi;
    end
else
    while phi<0
        phi=phi+2*pi;
    end
end
```

## INITIAL DISTRIBUTION LIST

	No. Copies
1. Defense Technical Information Center Cameron Station Alexandria, Virginia 22314-6145	2
2. Library, Code 52 Naval Postgraduate School Monterey, California 93943-5102	2
3. Dr. H.A. Titus, Code EC/Ts Department of Electrical and Computer Engineering Naval Postgraduate School Monterey, California 93943	5
4. Dr. J.B. Burl, Code EC/Bl Department of Electrical and Computer Engineering Naval Postgraduate School Monterey, California 93943	1
5. Dr. R. Cristi, Code EC/Cx Department of Electrical and Computer Engineering Naval Postgraduate School Monterey, California 93943	1
6. Dr. O. Heinz, Code PH/Hz Department of Physics Naval Postgraduate School Monterey, California 93943	1
7. Dr. I.M. Ross, Code AA/Ro Department of Aeronautics and Astronautics Naval Postgraduate School Monterey, California 93943	1
8. Dr. P.W. Schumacher, Jr. Analysis and Software Department U.S. Naval Space Surveillance Center Dahlgren, VA 22448	2